permafrost cci

CCI+ PHASE 1 – NEW ECVS

PERMAFROST

D4.1 PRODUCT VALIDATION AND INTERCOMPARISON REPORT (PVIR)

VERSION 2.0

30 SEPTEMBER 2020

PREPARED BY

b·geos

GAMMA REMOTE SENSING

UiO : University of Oslo

AWI

UNI FR
UNIVERSITÉ DE FRIBOURG
UNIVERSITÄT FREIBURG

Stockholm University

West University of Timisoara

TERRASIGNA

Document Status Sheet

Issue	Date	Details	Authors
1.0	30.09.2019	CRDPv0 evaluation	B. Heim, M. Wieczorek (AWI), A. Bartsch, C. Kroisleitner (B.GEOS) Cécile Pellet, Reynald Delaloye, Chloé Barboux (UNIFR)
2.0	30.09.2020	Update of all evaluation results based on CRDPv1	A. Bartsch (B.GEOS), B. Heim M. Wieczorek (AWI), Cécile Pellet, Reynald Delaloye (UNIFR)

Author team

Birgit Heim, AWI

Mareike Wieczorek, AWI

Cécile Pellet, UNIFR

Reynald Delaloye, UNIFR

Annett Bartsch, B.GEOS

Dan Jakober, B.GEOS

Georg Pointner, B.GEOS

Tazio Strozzi, GAMMA

ESA Technical Officer: Frank Martin Seifert

EUROPEAN SPACE AGENCY CONTRACT REPORT

The work described in this report was done under ESA contract. Responsibility for the contents resides in the authors or organizations that prepared it.

TABLE OF CONTENTS

EXECUTIVE SUMMARY

Within the European Space Agency (ESA), the Climate Change Initiative (CCI) is a global monitoring program, which aims to provide long-term Earth Observation (EO)-based Essential Climate Variables (ECVs) products to serve the climate modelling and climate user communities. Permafrost has been selected as one of the ECVs which are elaborated during Phase 1 of CCI+ (2018-2021). The required parameters by the Global Climate Observing System (GCOS)/World Meteorological Organisation (WMO) for the Permafrost ECVs are a) Permafrost temperature, and b) Thickness of the active layer.

The ECV Permafrost_cci products to be validated are: i) permafrost temperature, ii) active layer thickness, as well as iii) permafrost extent. The validation is carried out fully independent as the validation team is independent of the algorithm development team and uses the WMO Global Terrestrial Network for Permafrost (GTN-P), also specifically the mountain permafrost monitoring program PERMOS in Switzerland. The characterization of the errors and uncertainties that is described in this document is carried out using conventional evaluation of bias, absolute error and root mean square difference and binary match up analyses in comparison with the in situ measurements. Permafrost_cci also undertakes evaluation experiments in comparing Permafrost_cci permafrost temperature with the EO microwave derived Freeze-Thaw to Temperature (FT2T) product and for mountain permafrost areas using in situ ground surface temperature and rockglacier abundance.

The assessment results of the first Match-up based on the beta version of the Climate Research Data Package (CRDPv0) MAGT time series from 2003 to 2017 produced in phase 1 of the project in 2019 revealed that the warm temperature group >0 °C was outside of the Permafrost_cci MAGT value range and could, like this, not be included in the Match-up analyses. The Match-up analyses were performed for the cold temperature group with MAGT <1 °C revealing regional differences pointing to limitations due to the lack of representative information on ground stratigraphy. The Match-up for 2003 to 2017 for the Polar stereographic product (MAGT <1°C, depth 1, 2, 5 and 10 m) showed a bias of ~0.58°C and an RMSE of 1.41 °C.

In the second Match-up analyses, Permafrost_cci CRDPv1 (released in May 2020) MAGT time series from 1997 to 2018 show a good performance for the full temperature range including the warm temperature group above 0 °C. However, Permafrost_cci MAGT underestimation stays a characteristic of the warm temperature group. As a consequence of the cold bias in the warm temperature range, the binary match-up of "permafrost" versus "no permafrost" for Permafrost_cci PFR permafrost probability versus in situ MAGT ranges shows that PFR permafrost probability in the grid cell is overestimated compared to in situ-derived "no permafrost" and MAGT ≤0.5 °C. Permafrost_cci PFR permafrost probability in a grid cell with >0% occurs together with a wide range of "warm" in situ MAGT >0°C. The MAGT Match-up for the Polar stereographic product (POL, MAGT <1 °C, depth 1, 2, 5 and 10 m, n = 650) shows a bias of ~1.47 °C, an absolute bias of 1.64 °C, a RMSE of 1.89 °C, and a relative percentage error ($RPE_{5\text{-}95}$,within the 5% to 95% Quantile) of 80% for the time frame from 2003 to 2017 (as equivalent to the CRDPv0 time frame). The Match-up results for the Permafrost_cci MAGT CRDPv1 Polar stereographic product for the 1997 to 2018 records, providing more data (more regions, and by interpolation to 1 and 2 m depth, n = 924), show similar statistics with a bias of 1.14 °C, an absolute bias of 1.61 °C, a RMSE of 1.86 °C and a decrease in $RPE_{5\text{-}95}$ to 50%. Permafrost_cci MAGT CRDPv1 (MAGT <1 °C, all depths, n = 3186) in sinusoidal projection covering more measurement programmes in the subarctic and at mid latitudes shows the best performance with a warm bias of 1.05 °C, an absolute bias

of 1.54 °C, a RMSE of 1.85 °C and RPE_{5-95} of 38% . Permafrost_cci MAGT CRDPv1 is characterised by a too warm model bias for the cold temperature group (MAGT <1°C) in all model depths. Including the warm temperatures of MAGT ≥1 °C (n = 13695 match-up pairs) in the Match-up analyses results in a bias of -0.53 °C, an absolute bias of 1.33, an RMSE of 1.65 and an $RPE_{5\,95}$ of -16%.

PERMOS investigations in the Swiss Alps showed also a too warm model bias. Furthermore, the vast majority of inventoried ESA GlobPermafrost slope movement products are located outside of the simulated Permafrost_cci permafrost extent area and only four amongst the 10 PERMOS permafrost borehole sites are located within the simulated Permafrost_cci PFR permafrost extent area.

The comparison with FT2T freeze/thaw derived temperatures show specifically deviations in warm permafrost, in the transition zone.

Permafrost_cci ALT Match-up shows a moderate absolute bias of ~0.35 m and RMSE of ~0.50 m if calculated for the bulk data collection (CRDPv0 showed a RMSE ~1 m), a RPE_{5-95} of ~10% (within the 5% to 95% Quantile), and an absolute percentage error below 45%. Linear regression of Permafrost_cci ALT versus in situ ALT shows deviation from the 1:1 best fit in both directions: under- and overestimation of in situ ALT. One type of Permafrost_cci ALT underestimation of in situ ALT is linked to Arctic rock and stone desserts in Svalbard and Greenland. Permafrost_cci ALT overestimation on the other hand is visible at the southern boundaries of permafrost at mid-latitudes.

1 INTRODUCTION

ESA CCI is a global monitoring program, which aims to provide long-term EO-based ECV products to serve the climate modelling and climate user communities. Permafrost has been selected as one of the ECVs which are elaborated during Phase 1 of CCI+ (2018-2021). The required parameters by GCOS/ WMO for the Permafrost ECVs are a) Permafrost temperature (K), and b) Thickness of the active layer (m). Permafrost_cci added the variable: c) Permafrost extent as permafrost parameter, which is the areal fraction within a pixel at which the definition for the existence of permafrost (ground temperature <0 ºC for two consecutive years) is fulfilled.

A critical step in the acceptance of the CCI products by user communities is to provide a form of validation. The ECV Permafrost_cci products to be validated are: i) permafrost temperature, ii) active layer thickness, and iii) permafrost extent. EO-derived permafrost temperature forms the basis for calculation of the permafrost extent. The variable generation relies on the ground thermal model Permafrost_cci CryoGrid-3 (CC3) forced by EO-derived Land Surface Temperature (LST) and Snow Water Equivalent (SWE), with boundary conditions of EO-derived Land Cover. This novel ECV permafrost product will benefit a wide range of applications and users, thus a thorough user requirement analysis was performed at the beginning of the project.

The Committee on Earth Observing Satellites Working Group on Calibration and Validation (CEOS-WGCV) defines validation as 'the process of assessing, by independent means, the quality of the data products derived from the system outputs'. The GEO/CEOS Quality Assurance framework for Earth Observation (QA4EO) provides guidelines for the evaluation of EO-derived products. GEO/CEOS QA4EO expectations on Fiducial Reference Measurements (FRM) data sets are SI traceability using meteorological standards. On the other hand, for several geoscientific EO applications, accuracy is measured in terms of an agreement, or in terms of omission and commission errors. Therefore, if validation against precise FRM according to QA4EO criteria is not feasible, evaluation against suitable in-situ measurements is feasible or also evaluation against other sources using expert knowledge. According to QA4EO-criteria, validation needs to be independent from the retrieval process of the product. In the QA4EO sense, suitable validation data sets are characterised by measurement protocols and community-wide management practices and published openly. The validation data collection shall be a part of a collaborative user environment within an international framework. Within the Permafrost_cci validation framework we can guarantee independent validation, which is carried out with strong support of the user community; with in situ measurements characterised by community-wide management best practises with open data access and a collaborative user environment within an international framework: WMO and GCOS delegated the global monitoring of the ECV Permafrost to the Global Terrestrial Network for Permafrost (GTN-P) managed by the International Permafrost Association (IPA). GTN-P/IPA established the Thermal State of Permafrost Monitoring (TSP) for permafrost temperature monitoring and the Circumpolar Active Layer Monitoring program (CALM) for active layer thickness monitoring. Both GTN-P monitoring programs, TSP and CALM, require community standards for measurements and data collection and publish data sets on a) Permafrost temperature (K), and b) Thickness of active layer (m) (Biskaborn et al. 2015, 2019).

1.1 Purpose of the Document

The PVIR describes the assessments to evaluate the Climate Research Data Package CRDP Permafrost_cci products. The required parameters by GCOS for the Permafrost ECV are a) permafrost temperature, and b) active layer thickness. In many permafrost regions, these can have a high variability at spatial scales of meters, which is much finer than the footprint of EO-sensors. For this reason, Permafrost_cci provides an additional variable that is derived from Permafrost temperature: c) Permafrost extent (fraction), which is the areal fraction within an area (pixel) at which the definition for the existence of permafrost (ground temperature <0 ºC for two consecutive years) is fulfilled.

The generation of depth-specific ground temperature and thaw-depth time series relies on the ground thermal model Permafrost_cci CryoGrid 3, that is forced by EO-derived time series of LST and SWE with boundary conditions of EO-derived Land Cover. The variables of the Permafrost_cci CRDPv1 released in May 2020 comprise three time series:

1. simulated EO-forced 'mean annual Ground Temperature' (GTD) in 5 discrete depths (0 m, 1 m, 2 m, 5 m, 10 m) from 1997 to 2018
2. simulated EO-forced 'Active Layer Thickness' (ALT) from 1997 to 2018
3. 'Permafrost FRaction' (PFR) derived from GTD from 1997 to 2018.

The CRDPv1 product time series cover the Northern Hemisphere north of 30° N and are thus not global, e.g., permafrost in Antarctica is not yet covered. Hence, the PVIR in phase 2 assesses the Permafrost_cci products GTD 'permafrost temperature', ALT 'active layer thickness' and PFR 'Permafrost extent' in lowlands and mountain permafrost regions north of 30° N.

1.2 Structure of the Document

The PVIR is organised in 6 chapters.

- Chapter 1 provides the introduction and the overview on Permafrost_cci including applicable documents and the community glossary for Permafrost.
- Chapter 2 and its subsections describe the reference data sets and methods for the assessment of the variables: permafrost temperature, active layer thickness and permafrost extent.
- Chapters 3, 4, 5 present the results of the quality assessment for the Permafrost_cci products:
  - o Chapter 3 describes the quality assessment for Permafrost_cci permafrost temperature
  - o Chapter 4 describes the quality assessment for Permafrost_cci active layer thickness
  - o Chapter 5 describes the quality assessment for Permafrost_cci permafrost extent
- Chapter 6 provides a summary and recommendations.

1.3 Applicable Documents

[AD-1] ESA 2017: Climate Change Initiative Extension (CCI+) Phase 1 – New Essential Climate Variables - Statement of Work. ESA-CCI-PRGM-EOPS-SW-17-0032

[AD-2] Requirements for monitoring of permafrost in Polar Regions - A community white paper in response to the WMO Polar Space Task Group (PSTG), Version 4, 2014-10-09. Austrian Polar Research Institute, Vienna, Austria, 20 pp

[AD-3] ECV 9 Permafrost: assessment report on available methodological standards and guides, 1 Nov 2009, GTOS-62

[AD-4] GCOS-200, the Global Observing System for Climate: Implementation Needs (2016 GCOS Implementation Plan, 2015.

1.4 Reference Documents

[RD-1] Bartsch, A.; Grosse, G.; Kääb, A.; Westermann, S.; Strozzi, T.; Wiesmann, A.; Duguay, C.; Seifert, F. M.; Obu, J.; Goler, R.: GlobPermafrost – How space-based earth observation supports understanding of permafrost. Proceedings of the ESA Living Planet Symposium, pp. 6.

[RD-2] Bartsch, A.; Grosse, G.; Kääb, A.; Westermann, S.; Strozzi, T.; Wiesmann, A.; Duguay, C.; Seifert, F. M.; Obu, J.; Goler, R.: GlobPermafrost – How space-based earth observation supports understanding of permafrost. Proceedings of the ESA Living Planet Symposium, pp. 6.

[RD-3] Bartsch, A., Westermann, Strozzi, T., Wiesmann, A., Kroisleitner, C. (2019): ESA CCI+ Permafrost Product Specifications Document, v1.0

[RD-4] Bartsch, A., Matthes, H., Westermann, S., Heim, B., Pellet, C., Onacu, A., Kroisleitner, C., Strozzi, T. (2019): ESA CCI+ Permafrost User Requirements Document, v1.0

[RD-5] Bartsch, A., Westermann, S., Heim, B., Wieczorek, M., Pellet, C., Barboux, C., Kroisleitner, C., Strozzi, T. (2019): ESA CCI+ Permafrost Data Access Requirements Document, v1.0

[RD-6] Heim, B., Wieczorek, M., Pellet, C., Barboux, C., Delaloye, R., Bartsch, A, Strozzi, T. (2019): ESA CCI+ Product Validation Plan, v1.0

[RD-7] Heim, B., Wieczorek, M., Pellet, C., Barboux, C., Delaloye, R., Bartsch, A., Strozzi, T. (2019): ESA CCI+ PVIR, v1.0

1.5 Bibliography

A complete bibliographic list that support arguments or statements made within the current document is provided in Section 6.1.

1.6 Acronyms

A list of acronyms is provided in section 7.2.

1.7 Glossary

The list below provides a selection of terms relevant for the parameters addressed in Permafrost_cci [AD-1]. A comprehensive glossary is available as part of the Product Specifications Document [RD-4].

active-layer thickness

The thickness of the layer of the ground that is subject to annual thawing and freezing in areas underlain by permafrost.

The thickness of the active layer depends on such factors as the ambient air temperature, vegetation, drainage, soil or rock type and total water content, snowcover, and degree and orientation of slope. As a rule, the active layer is thin in the High Arctic (it can be less than 15 cm) and becomes thicker farther south (1 m or more).

The thickness of the active layer can vary from year to year, primarily due to variations in the mean annual air temperature, distribution of soil moisture, and snowcover.

The thickness of the active layer includes the uppermost part of the permafrost wherever either the salinity or clay content of the permafrost allows it to thaw and refreeze annually, even though the material remains cryotic (T <0 °C).

Use of the term "depth to permafrost" as a synonym for the thickness of the active layer is misleading, especially in areas where the active layer is separated from the permafrost by a residual thaw layer, that is, by a thawed or noncryotic (T >0 °C) layer of ground.

REFERENCES: Muller, 1943; Williams, 1965; van Everdingen, 1985

continuous permafrost

Permafrost occurring everywhere beneath the exposed land surface throughout a geographic region with the exception of widely scattered sites, such as newly deposited unconsolidated sediments, where the climate has just begun to impose its influence on the thermal regime of the ground, causing the development of continuous permafrost.

For practical purposes, the existence of small taliks within continuous permafrost has to be recognized. The term, therefore, generally refers to areas where more than 90 percent of the ground surface is underlain by permafrost.

REFERENCE: Brown, 1970.

discontinuous permafrost

Permafrost occurring in some areas beneath the exposed land surface throughout a geographic region where other areas are free of permafrost.

Discontinuous permafrost occurs between the continuous permafrost zone and the southern latitudinal limit of permafrost in lowlands. Depending on the scale of mapping, several subzones can often be distinguished, based on the percentage (or fraction) of the land surface underlain by permafrost, as shown in the following table.

Permafrost	English usage	Russian Usage
Extensive	65-90%	Massive Island
Intermediate	35-65%	Island
Sporadic	10-35%	Sporadic
Isolated Patches	0-10%	-

SYNONYMS: (not recommended) insular permafrost; island permafrost; scattered permafrost.
REFERENCES: Brown, 1970; Kudryavtsev, 1978; Heginbottom, 1984; Heginbottom and Radburn, 1992; Brown et al., 1997.

mean annual ground temperature (MAGT)

Mean annual temperature of the ground at a particular depth.
The mean annual temperature of the ground usually increases with depth below the surface. In some northern areas, however, it is not un-common to find that the mean annual ground temperature decreases in the upper 50 to 100 metres below the ground surface as a result of past changes in surface and climate conditions. Below that depth, it will increase as a result of the geothermal heat flux from the interior of the earth. The mean annual ground temperature at the depth of zero annual amplitude is often used to assess the thermal regime of the ground at various locations. [RD-7]

permafrost

Ground (soil or rock and included ice and organic material) that remains at or below 0°C for at least two consecutive years .
Permafrost is synonymous with perennially cryotic ground: it is defined on the basis of temperature. It is not necessarily frozen, because the freezing point of the included water may be depressed several degrees below 0°C; moisture in the form of water or ice may or may not be present. In other words, whereas all perennially frozen ground is permafrost, not all permafrost is perennially frozen. Permafrost should not be regarded as permanent, because natural or man-made changes in the climate or terrain may cause the temperature of the ground to rise above 0 °C.
Permafrost includes perennial ground ice, but not glacier ice or icings, or bodies of surface water with temperatures perennially below 0°C; it does include man-made perennially frozen ground around or below chilled pipe-lines, hockey arenas, etc.
Russian usage requires the continuous existence of temperatures below 0 °C for at least three years, and also the presence of at least some ice.
SYNONYMS: perennially frozen ground, perennially cryotic ground and (not recommended) biennially frozen ground, climafrost, cryic layer, permanently frozen ground.
REFERENCES: Muller, 1943; van Everdingen, 1976; Kudryavtsev, 1978.

2 METHODS FOR QUALITY ASSESSMENT

This chapter provides an overview on the assessment of the performance of the Permafrost_cci products. The PVIR structure is organised according to the Permafrost_cci products to be validated: Permafrost_cci CryoGrid-3 permafrost temperature (GTD), active layer thickness (ALT) and permafrost extent (PFR) [RD-3]. Special emphasis in Permafrost_cci is placed on validation using data from international and national permafrost monitoring networks and in cooperation with the permafrost community. Within Permafrost_cci, we compiled a new substantial Match-up data collection from the main community (permafrost, meteorology) pre-existing in situ data sets. These available in situ data sets, the data characteristics and data availability (data access via data portals, repositories and program websites) are described in detail in the Permafrost_cci DARD [RD-5] and PVP [RD-6] reports.

WMO and GCOS delegated the ground-based monitoring of the ECV Permafrost to GTN-P/IPA, who established TSP and CALM. The national-wide Russian meteorological monitoring network ROSHYDROMET provides in addition long-term ground temperature records close to meteorological stations. GTN-P and ROSHYDROMET time series and data collections from additional networks provide ground-based climate record data sets, however no easy-to use or readily available time-series depth data that are data-fit for validation and round robin exercises. To validate the Permafrost_cci products, Permafrost_cci needed to optimise the GTN-P/IPA, ROSHYDROMET and other in situ data collections. For example, the data collection of ground-temperature time series is a highly complex and heterogeneous data set including variable timeframes from hourly over annually to sporadic measurements, in different depths and not consistent over time. In addition, all the data collections contain quite a large amount of incomplete and erroneous data, including erroneous or imprecise coordinate locations, depending on region and principal investigators. Within the framework of Permafrost_cci, the pre-existing community in situ data sets have been error-checked, corrected, homogenised, filtered and standardised. The newly compiled, harmonised Permafrost_cci set of ground temperature depth-time series provides the first consistent data collection usable for evaluation of ground temperature in the circum-Arctic. It covers all permafrost zones from continuous to discontinuous, sporadic and isolated. The new harmonised ground temperature data set is a data collection with all available measurement depths down to 20 m. In addition, Permafrost_cci specifically assembled ground temperature data in shallow depths down to 5 m to provide simulation data for climate and land surface models.

Permafrost_cci retrieval skills are evaluated using pixel-based Match-up analyses and additionally more complex combinations using expert knowledge. The first product quality assessment is described in detail in the PVIR v1 [RD-7]. The validation and evaluation efforts also include innovatively applied EO microwave-derived ground temperature, the Freeze-Thaw to Temperature (FT2T) product for comparison with the Permafrost_cci permafrost temperature product. GTN-P PERMOS in Switzerland is assessing the Permafrost_cci permafrost temperature and permafrost extent products in high-mountain permafrost regions, using in situ observations of surface temperature and borehole ground temperatures and the ESA GlobPermafrost rock glacier inventory.

Permafrost_cci entirely acknowledges the efforts of the international permafrost community in this impressive realization of circumpolar measurements, and all national initiatives from Russia, US, Canada, Switzerland and Norway for making the measurement data publicly available.

2.1 Pair-wise Match-Up Evaluation

We constructed a pixel-based pair-wise Permafrost_cci Match-up data collection based on

i) *standardised in situ ground temperature (GT) data from 1997 to 2018 with a circum-Arctic geographic coverage*, providing mean annual ground temperature (MAGT) in discrete measurement depths per year. This data collection is assembled as merged and newly standardised data from the community GT data archives across all permafrost zones (continuous, discontinuous, sporadic, and isolated). We also use the in situ MAGT time series for the binary evaluation of permafrost abundance.
Reference in situ data sets provided for the Match-up evaluation are

- in situ MAGT [Latitude, Longitude] in discrete depths in annual resolution from 1997 to 2018
- in situ PFR [Latitude, Longitude] permafrost probability in annual resolution from 1997 to 2018

ii) *standardised in situ active layer thickness (ALT) data from 1997 to 2018 with a circum-Arctic geographic coverage*. We also use the ALT time series for a binary evaluation of permafrost abundance.
This in situ data collection covers the continuous Permafrost zone.
Reference in situ data sets provided for the Match-up evaluation are

- in situ ALT [Latitude, Longitude] in annual resolution from 1997 to 2018
- in situ PFR [Latitude, Longitude] permafrost probability in annual resolution from 1997 to 2018

iii) *Permafrost_cci CRDPv1*, which is the 2nd product release and was issued in May 2020. Permafrost_cci CRDPv1 provides 1 km pixel resolution ECV products on MAGT at discrete ground depths (0, 1, 2, 5, 10 m), Active Layer Thickness (ALT) and Permafrost Extent (PFR; permafrost probability) in Polar stereographic projection, named Permafrost_cci POL.
Part of the Match up analyses in this study are also carried out with the pre-release version in original sinusoidal projection based on MODIS tile format, named Permafrost_cci SIN. The differences between extracted variable values from the two products are due to the different geometry and pixel infilling for spatial extrapolation in case of the stereographic circumpolar projection, specifically at high latitudes; however, differences of extracted variable values are minor in most of the regions. Permafrost_cci SIN is compiled for discrete depths at the locations of the in situ measurements of the Permafrost_cci reference data collection: extracted data are at depths 0, 0.2, 0.25, 0.4, 0.5, 0.6, 0.75, 0.8, 1.0, 1.2, 1.6, 2.0, 2.4, 2.5, 3.0, 3.2, 4.0, 5.0, 10.0 m.

- Permafrost_cci MAGT (GTD) POL [Latitude, Longitude] in discrete depths (0, 1, 2, 5, 10 m) in annual resolution from 1997 to 2018.
- Permafrost_cci MAGT (GTD) SIN [Latitude, Longitude] in discrete depths (0, 0.2, 0.25, 0.4, 0.5, 0.6, 0.75, 0.8, 1.0, 1.2, 1.6, 2.0, 2.4, 2.5, 3.0, 3.2, 4.0, 5.0, 10.0 m) in annual resolution from 1997 to 2018.
- Permafrost_cci ALT POL and SIN [Latitude, Longitude] in annual resolution from 1997 to 2018.
- Permafrost_cci PFR POL [Latitude, Longitude] permafrost probability (extracted at 2 m depth) in annual resolution from 1997 to 2018.

The objective of this time- and depth-specific Match-up is to compare the simulated variables with the in situ measured variables in order to assess the extent to which the Permafrost_cci GryoGrid-3 simulation is able to represent the in-situ measurements in each year. The Permafrost_cci simulation is forced by coarse-scale satellite data products and thus represents a landscape scale in form of a weighted average over a larger area of kilometres. The in situ measurements on the other hand, i.e., the borehole locations and the 100 m×100 m CALM grid active layer measurements are confined to a small local area. In contrast, the gridded satellite observations and reanalysis data of LST and SWE map a grid with coarse km-scale resolution on a defined Earth surface. Already with the Permafrost_cci sinusoidal SIN product geometry, each in situ measurement is moved further away from its original location to a nearby location on the map grid. The Polar stereographic projection requires pixel infilling and further smooths out landscape heterogeneity in comparison to the SIN product. The comparison of discrete depths further compromises the precision in case of shallow depth specifically, as permafrost landscapes are frequently characterised by a heterogeneous micro-topography, leading to an inconsistent depth extrapolation for shallow depths.

The Permafrost_cci in situ reference data collections of MAGT and ALT are characterised by spatial and temporal biases related to regions, time covered and measurement depths due to the high variety in national measurement programs, principal investigators and funding sources. This results in a large variability of Permafrost_cci reference in situ Match-up pairs in time, region and for example, MAGT reference depths.

For all these reasons, a Match-up analysis with the produced reference data sets can only provide an estimate of accuracy rather than a thorough error analyses. However, Match-up analyses are adequate assessment tools to link the statistic Match-up performance to regions, characteristics of the data sets and processes occurring in permafrost landscapes. For this reason, Permafrost_cci undertakes the pixel-based comparison between the simulated Permafrost_cci products MAGT, ALT and PFR products and in situ measurements at individual stations relying on statistical metrics for its common usage.

The following listing describes statistics terms and codes in all the assessments used in Permafrost_cci: number of measurements (*n*), standard deviation (*sd*), maximum value (*max*), minimum value (*min*), slope of the best linear fit equation (*S*), intercept of the best linear fit equation (*I*), coefficient of correlation (r^2), relative bias (*bias*), absolute bias (*abs_bias*) relative root mean square error (*RMSE)*, mean absolute percentage error *(APE)*, relative percentage error *(RPE).*

The *bias* is the mean deviation of the product to the in situ data and calculated by

$$bias = \frac{\sum_{i=1}^{n}(Permafrost_{cci} - in\ situ)}{n}$$

This results in a positive bias if the product is too warm and vice versa. Given that large deviations in positive and negative direction can result in a bias ~0, we additionally use the absolute bias (*abs_bias*), calculated by

$$abs\_bias = \frac{\sum_{i=1}^{n}|(Permafrost_{cci} - in\ situ)|}{n}$$

The residual mean square error (RMSE) is calculated by

$$RMSE = \sqrt{\frac{\sum_{i=1}^{n}(Permafrost_{cci} - in\ situ)^2}{n}}$$

Additional statistics provided are the relative percentage error (*RPE*) and the absolute percentage error (*APE*). The RPE is calculated by

$$RPE = \frac{\sum_{i=1}^{n}\frac{(Permafrost_{cci} - in\ situ)}{|in\ situ|}}{n} * 100$$

By using the absolute value, we ensure that the *bias* defines the sign of the *RPE*. The *APE* is then calculated by using the absolute values

$$APE = \frac{\sum_{i=1}^{n}\left|\frac{(Permafrost_{cci} - in\ situ)}{|in\ situ|}\right|}{n} * 100$$

Both, RPE and APE have very high values if the in situ temperature is very small and if data outliers are abundant. We thus additionally show RPE and APE within their specific ranges between the 5% and 95% Quantiles ($RPE_{5\text{-}95}$ and $APE_{5\text{-}95}$) to minimize the influence of data outliers.

2.2 Assessment of Permafrost Temperature

2.2.1 In Situ Ground Temperature Reference Data Generation

Version 2 synthesised permafrost temperature - discrete depths

Permafrost_cci match-up data set in phase 2, Version 2: standardised ground temperature per depth GTD data with annual resolution from 1997 and 2018 with a circum-Arctic geographic coverage.
This mean annual GTD data set from 1997 to 2018 is compiled from all the discrete depths and time stamps and national and international programs available: depths are at 0, 0.2, 0.25, 0.4, 0.5, 0.6, 0.75, 0.8, 1.0, 1.2, 1.6, 2.0, 2.4, 2.5, 3.0, 3.2, 4.0, 5.0, 10.0, 15.0, 20.0 m. The complete data set has been compiled from

- GTN-P (https://gtnp.arcticportal.org/) [global monitoring programme]
- Roshydromet RHM (http://meteo.ru/data/164-soil-temperature) [national monitoring programme, Russia]
- Nordicana-D [world data repository for Polar research, Canada] (http://www.cen.ulaval.ca/nordicanad/dpage.aspx?doi=45291SL34F28A9491014AFD; Allard et al., 2016, CEN 2013),
- PANGAEA [world data repository for environmental research, Germany] (https://doi.pangaea.de/10.1594/PANGAEA.905233; Boike et. al. 2019; https://doi.pangaea.de/10.1594/PANGAEA.884711, GTN-P 2018, https://doi.pangaea.de/10.1594/PANGAEA.912482, Bergstedt & Bartsch 2020,
- Arctic Data Center [world data repository for Polar research, United States] (https://arcticdata.io/catalog/ #view/doi:10.18739/A2KG55; Wang et al. 2018)
- from individual members of the Permafrost research community (V. Romanovski & A. Kholodov (GTN-P, University of Alaska Fairbanks (UAF), US), M. Ulrich (University of Leipzig, DE)).

This Permafrost_cci GT Match-up data collection contains data from 300 in situ measurement locations (GTN-P n = 66, RHM n = 151, Nordicana-D n = 5, PANGAEA n = 15, Arctic Data Center n = 66, PIs = 7), with overall n = 13695 match-up pairs in time and depth (depths ≤10 m, Ø ~ 720 values per depth). 142 in situ measurement locations with 3185 match-up pairs in time and depth fall into the match-up group of mean annual GT <1 °C.

For Permafrost_cci purposes it was required to carry out coordinate corrections, outlier and error elimination. We treated shallow and deep ground temperature measurements differently and provide the synthesised GT data sets as two different GT data collections:

- *Group I* shallow GT measurement depth profiles going down to 5 m depth (exclusive). In Group I, all discrete values were calculated.

- *Group II* GT measurement depth profiles of 5 m depth and deeper. Within Group II, we discarded all data <2 m depth from deep boreholes as in borehole with large diameters, there is either frequently artificial material in-filling or air, resulting in not adequate ground temperature measurements. Data <2 m were only kept if confirmed reliable by the PI.

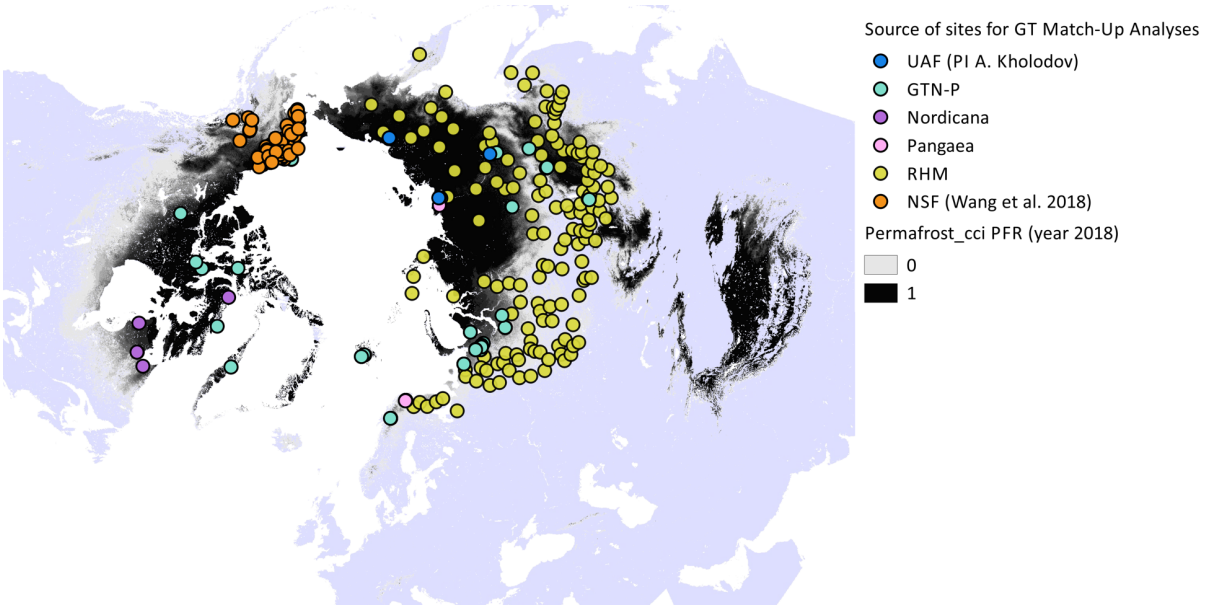

Figure 2.1. Northern hemisphere Permafrost_cci PFR permafrost probability and in situ ground temperature stations (grouped by data source).

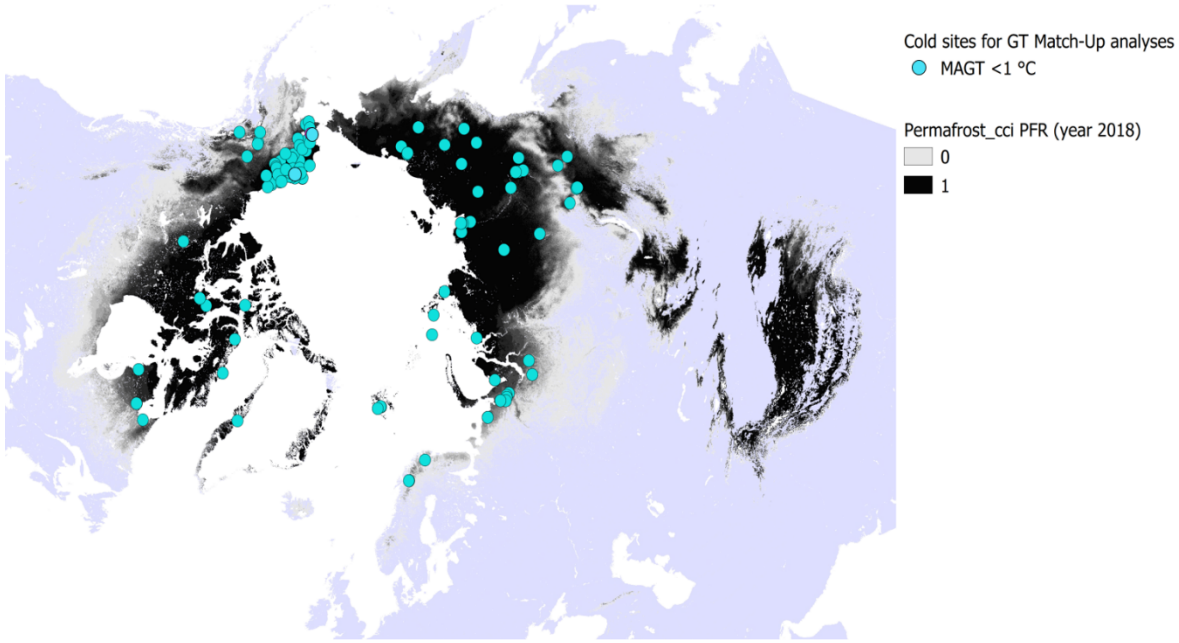

Figure 2.2. Northern hemisphere Permafrost_cci PFR permafrost probability and in situ ground temperature stations with MAGT <1 °C.

GT data were processed to yearly Mean Annual Ground Temperature (MAGT), containing metadata information, which allows assessing the quality of each temperature value product. These metadata comprise for yearly values the ratio of missing data per month/year (missing days per year/365) and the amount of completely missing months. Yearly means are not calculated if >20% of yearly values are not available or if more than one complete month is missing. An exception is made for the data of GTN-P (2018) which represent temperature at the depth of Zero Annual Amplitude (ZAA) and are kept although only one value per year is available.

Table 2.1. Example of how the compiled data set provides the metadata information of the yearly values. Mxx = ratio of missing values per month/year at depth xx m. mMxx = number of completely missing months per year at depth xx m.

	Site	Year	Type	M0	M0.2	M0.25	M0.4	M0.5	M0.75	M0.8	M1	mM0	mM0.2	mM0.2	mM0.4	mM0.5	mM0.7	mM0.8	mM1	0	0.2	0.25	0.4	0.5	0.75	0.8	1
2	FB_dry_l	2006	Mean	1	1	1	1	1	1	1	1	12	12	12	12	12	12	12	12	NA	NA	NA	NA	NA	NA	NA	NA
3	FB_dry_l	2006	Max	1	1	1	1	1	1	1	1	12	12	12	12	12	12	12	12	NA	NA	NA	NA	NA	NA	NA	NA
4	FB_dry_l	2006	Min	1	1	1	1	1	1	1	1	12	12	12	12	12	12	12	12	NA	NA	NA	NA	NA	NA	NA	NA
5	FB_wet_	2006	Mean	0.414	0.414	0.414	0.416	0.414	NA	NA	NA	5	5	5	5	0	NA	NA	NA	1.33	1.64	1.56	1.35	1.12	NA	NA	NA
6	FB_wet_	2006	Max	0.414	0.414	0.414	0.416	0.414	NA	NA	NA	5	5	5	5	0	NA	NA	NA	18.9	12.7	12	10.4	8.07	NA	NA	NA
7	FB_wet_	2006	Min	0.414	0.414	0.414	0.416	0.414	NA	NA	NA	5	5	5	5	0	NA	NA	NA	-19.1	-12	-11.5	-10.2	-8.95	NA	NA	NA
8	FB_dry_l	2007	Mean	0.581	0.581	0.581	0.581	0.581	1	0.586	0.699	7	7	7	7	7	12	7	8	-3.58	-2.65	-2.53	-2.38	-2.44	NA	-2.4	-2.59
9	FB_dry_l	2007	Max	0.581	0.581	0.581	0.581	0.581	1	0.586	0.699	7	7	7	7	7	12	7	8	13.6	10.4	9.31	8.01	4.87	NA	1.73	0.63
10	FB_dry_l	2007	Min	0.581	0.581	0.581	0.581	0.581	1	0.586	0.699	7	7	7	7	7	12	7	8	-21.9	-17.5	-16.9	-16	-14.6	NA	-11.9	-8.83
11	FB_wet_	2007	Mean	0	0	0	0	0	NA	NA	NA	0	0	0	0	0	NA	NA	NA	-5.99	-5.41	-5.62	-5.48	-5.63	NA	NA	NA
12	FB_wet_	2007	Max	0	0	0	0	0	NA	NA	NA	0	0	0	0	0	NA	NA	NA	17.8	15.2	11.7	10.6	7.49	NA	NA	NA
13	FB_wet	2007	Min	0	0	0	0	0	NA	NA	NA	0	0	0	0	0	NA	NA	NA	-30.2	-23.3	-22.7	-21.3	-20.3	NA	NA	NA

2.2.2 Characteristics of Ground Temperature Match-up Data Set

The in situ reference data collection 'synthesised GT at discrete depths' with overall n = 13695 Match-up pairs in time and depth from 300 sites contains a large group of boreholes with MAGT >0 °C, as several boreholes were specifically sampled along the southern boundary of the "isolated permafrost" zone.

Exclusion of non-permafrost temperatures in GT Match-up Data Set v1 (Validation in phase 1, CRDPv0 2019)

For straightforward Match-up analyses in the first validation round [RD-7], we evaluated only permafrost temperature and not ground temperature in general. Therefore, we excluded all stations with in situ measurements of MAGT ≥1 °C at least once (independent of measurement depth) from the match-up analyses. This GTD Match-up dataset, with all 'warm temperature' station types excluded, contained only n = 3185 match-up pairs in time and depth. The new assessment (as detailed below) includes non-permafrost sites and considers more than 10.000 match-up pairs.

Inclusion of warm temperatures, exclusion of high mountain, mountain top and Yedoma boreholes in GT Match-up Data Set v2 (Validation in phase 2, CRDPv1 2020)

We conduct the second validation round in phase 2 using
i) the GTD data collection with also the 'non-permafrost' ground temperature with MAGT ≥1 °C included (depths down to 10 m). This GTD Match-up data set for Permafrost_cci MAGT SIN in 0, 0.2, 0.25, 0.4, 0.5, 0.6, 0.75, 0.8, 1.0, 1.2, 1.6, 2.0, 2.4, 2.5, 3.0, 3.2, 4.0, 5.0, 10.0 m depth includes n = 13695 Match-up pairs in time and depth and Permafrost_cci MAGT POL in 0, 1, 2, 5, 10 m depth includes n = 813 Match-up pairs in time and depth.

We also conduct Match-up analyses with focus on permafrost temperature using
ii) the GTD data collection restricted to MAGT <1 °C (depths down to 10 m).
This GTD Match-up data set includes n = 3186 Match-up pairs in time and depth for Permafrost_cci MAGT SIN in 0, 0.2, 0.25, 0.4, 0.5, 0.6, 0.75, 0.8, 1.0, 1.2, 1.6, 2.0, 2.4, 2.5, 3.0, 3.2, 4.0, 5.0, 10.0 m depth and n = 767 Match-up pairs in time and depth for Permafrost_cci MAGT POL in 0, 1, 2, 5, 10 m depth.

As especially the Russian boreholes have only few measurements at exactly 1 or 2 m depth, we started interpolating temperature values for the Permafrost_cci focus depths. To achieve this, we only use sites with at least three sensors in the lower depth down to 1.20 m. Interpolation was conducted by linear regression between two single measurement depths, resulting in separate equations for each sensor-pair and year.

Please note that we excluded all sites that are not representative of the landscape-scale of in-situ measurements from all three Match-up data collections: these are mountain sites (n = 18) that are specifically assessed by PERMOS, small-scale landscape anomalies such as very local peatland patches or in-situ measurements in pingos (ice hills, n = 3). Please also note that we excluded all sites within the Siberian Yedoma area (shape file from Bryant et al., 2017) due to incorrect parameterisation of Permafrost_cci CryoGrid-3 of Yedoma stratigraphy (n = 7).

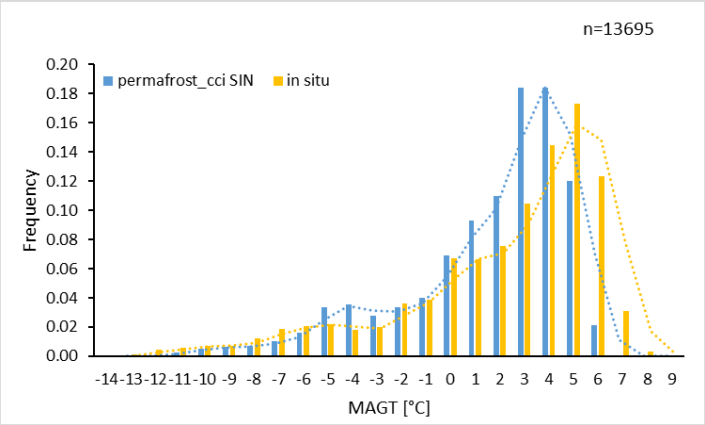

Figure 2.3. Frequency distribution of the Match-up data collection v2 (2020), all sites, n = 13695. In situ data at all discrete depths ≤10 m and Permafrost_cci MAGT SIN is given in ranges with steps of 1 °C. Excluded are 3 sites which are anomalies on the landscape scale, 15 sites in high mountain areas, 3 sites on arctic mountain tops, and 7 sites within Siberian Yedoma (shape file from Bryant et al., 2017).

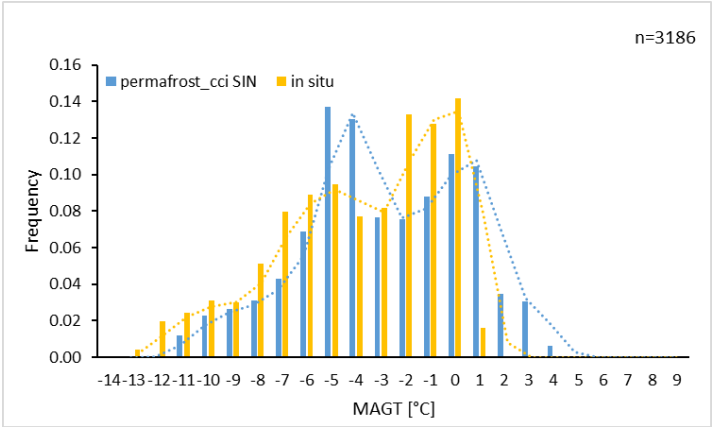

Figure 2.4. Frequency distribution of the Match-up data collection v2 (2020), with sites with in situ MAGT ≥1 °C excluded, n = 3186. In situ data at all discrete depths ≤10 m and Permafrost_cci MAGT SIN is given in ranges with steps of 1 °C. Excluded are sites which are anomalies on the landscape scale, sites in high mountain areas and on arctic mountain tops, and sites within Siberian Yedoma (shape file from Bryant et al., 2017).

The GTD Match-up v2 (2020) contains the cleaned and interpolated in situ reference data collection of synthesised MAGT at discrete depths matched with CRDPv1 Permafrost_cci MAGT SIN in 0, 0.2, 0.25, 0.4, 0.5, 0.6, 0.75, 0.8, 1.0, 1.2, 1.6, 2.0, 2.4, 2.5, 3.0, 3.2, 4.0, 5.0, 10.0 m, and Permafrost_cci MAGT POL in 0, 1, 2, 5, 10 m depth. Figure 2.3 shows the frequency distribution of the Match up data set with n = 13695, Figure 2.4 with in situ MAGT ≥1 °C excluded, with n = 3186.

The characteristics of Permafrost_cci MAGT SIN (Figures 2.3, 2.4) show a bimodal distribution. A first Permafrost_cci MAGT SIN peak arises around –5 to –4 °C. A second peak in Permafrost_cci MAGT SIN appears between 3 and 4 °C, whereas in situ MAGT peaks with 1 °C warmer temperature around 5 °C. Permafrost_cci MAGT SIN shows more abundance of colder MAGT values. In the MAGT data group <1 °C the highest frequency of Permafrost_cci MAGT SIN is around –5 to –4 °C whereas in situ MAGT shows high frequency around –2 to 0 °C.

Permafrost_cci MAGT POL is similar to Permafrost_cci MAGT SIN with some exceptions at spatially heterogeneous sites where Permafrost_cci MAGT POL shows less spatial details and appears more averaged over the landscape scale that becomes more prominent in the southern permafrost zones at warmer ground temperatures (Figure 2.5)

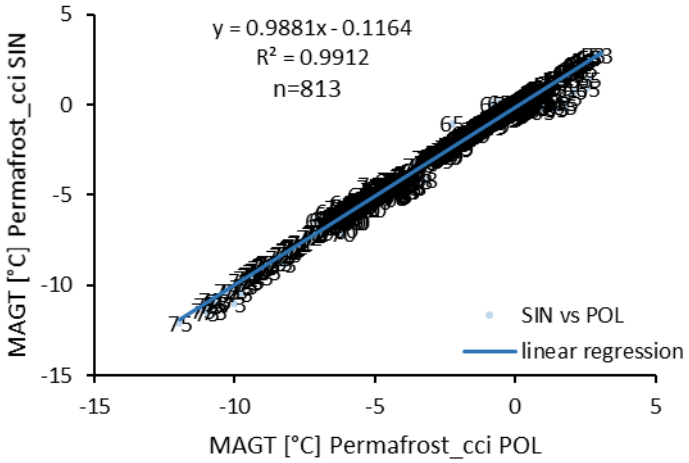

Figure 2.5. Comparison of Permafrost_cci MAGT SIN vs. Permafrost_cci MAGT POL at Match-up sites. Labels show latitude.

The characteristics of Permafrost_cci MAGT POL Match-up data set (constrained to in situ MAGT <1 °C), with n = 813 (Figure 2.6) shows a similar bimodal distribution with a first Permafrost_cci MAGT peak around –6 °C and highest abundance at relative warm MAGT around 0 °C. RHM in situ data are not represented in this Match-up data collection due to different measurement depths. Interpolated in situ data, including RHM sites in the POL Match-up, are presented in Figure 2.7 and mostly resemble those of Figure 2.6. In general, GT data from the data archives of GTN-P, Nordicana-D, and the Arctic Data Center cover more colder sites at higher latitudes (e.g., Figure 2.1, 2.8) than RHM that is more represented in the southern permafrost zones (e.g., Figure 2.1, 2.9).

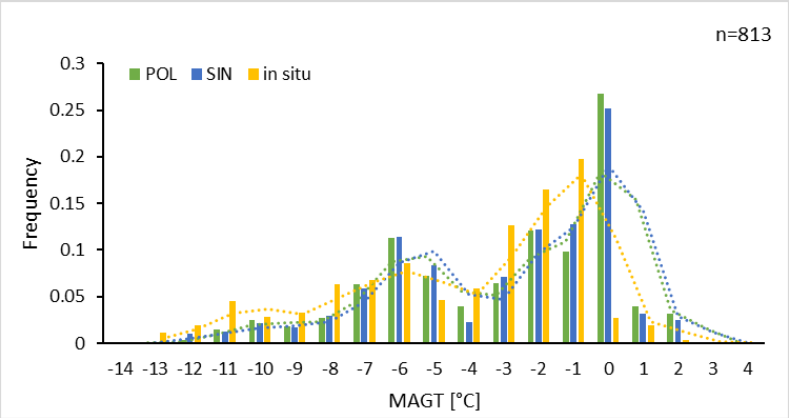

Figure 2.6. Frequency distribution of the Match-up data collection v2 (2020) confined to Match-up pairs in the five Permafrost_cci product depths (0, 1, 2, 5, 10 m), n = 813. In situ data at all discrete depths 0, 1, 2, 5, 10 m and Permafrost_cci MAGT POL and SIN is given in ranges with steps of 1 °C. Excluded are sites which are anomalies on the landscape scale, sites in high mountain areas and on arctic mountain tops, and sites within Siberian Yedoma (shape file from Bryant et al., 2017).

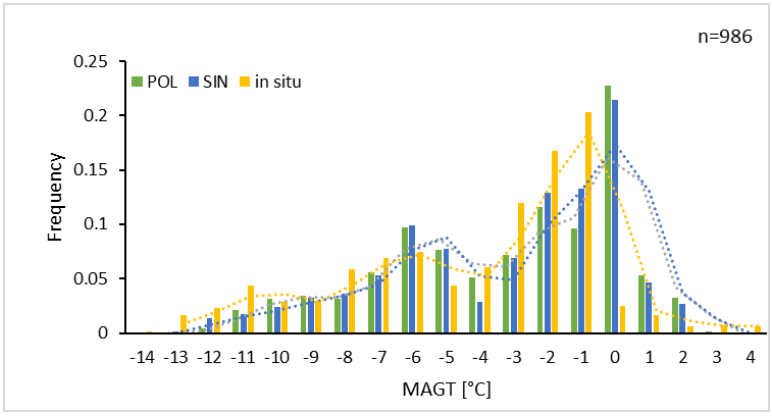

*Figure 2.7. Frequency distribution of the Match-up data collection v2 (2020) confined to Match-up pairs in the five Permafrost_cci product depths (0, 1, 2, 5, 10 m) with more Match-up pairs by **interpolation** of in situ data to 1 and 2 m depth , n = 986. In situ data at all discrete measurement depths 0, 1, 2, 5, 10 m with additional **interpolated** data at shallow depths of 1 m and 2 m and Permafrost_cci MAGT POL and SIN is given in ranges with steps of 1 °C. Excluded are sites which are anomalies on the landscape scale, sites in high mountain areas and on arctic mountain tops, and sites within Siberian Yedoma (shape file from Bryant et al., 2017).*

Figure 2.8 shows the frequency distribution of the data collections of GTN-P, Wang et al. (2018) and NORDICANA-D in the depths of 0.75, 1 and 2 m, which are mainly located in the circum-Arctic, but also including mid latitudes. Figure 2.9 shows the frequency distribution of mainly ROSHYDROMET in situ MAGT, containing much fewer boreholes at high latitudes but mainly covering the mid latitudes with main contributions to depths of 0.80, 1.20, 2.40 m.

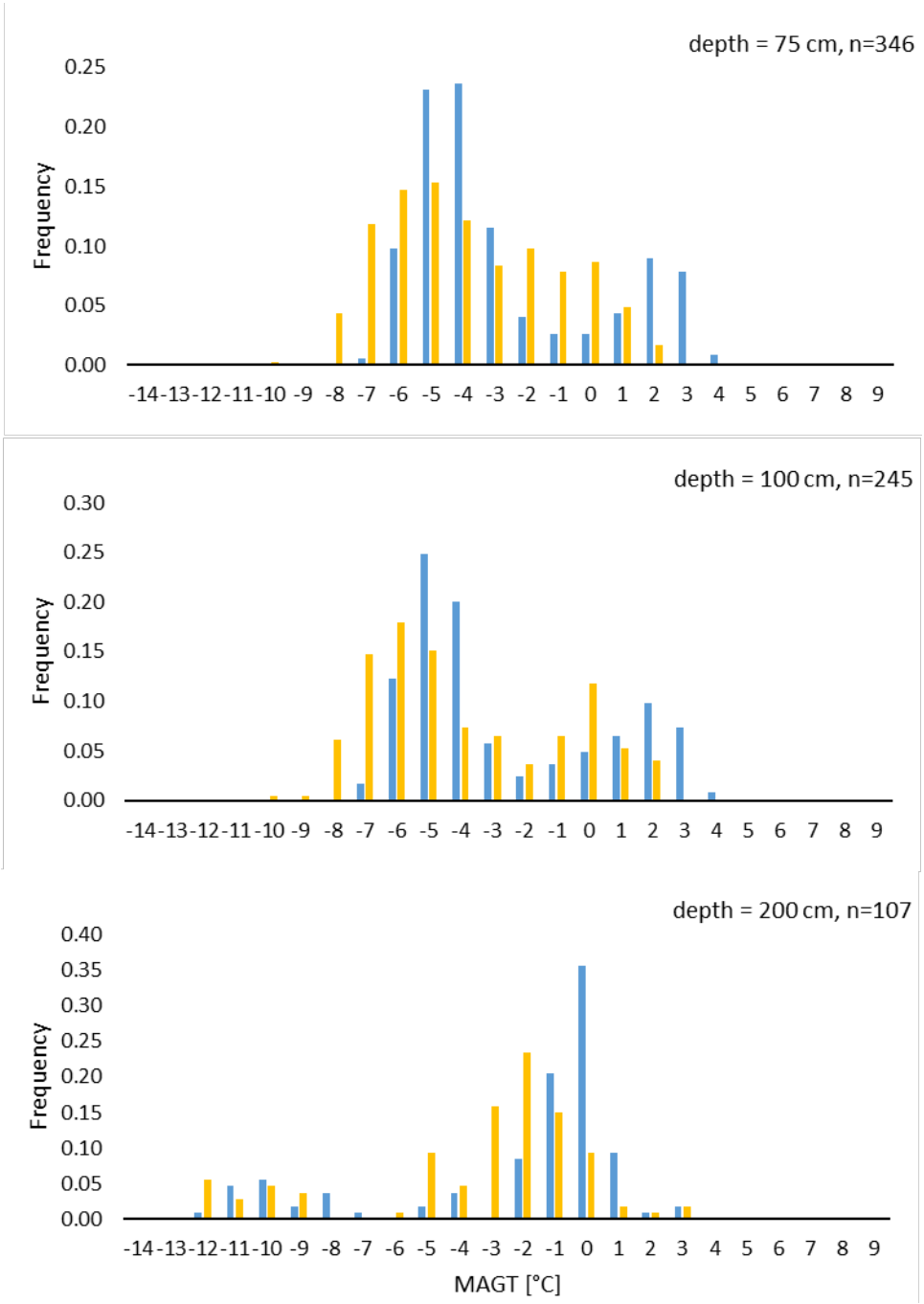

Figure 2.8. Frequency distribution of the Match-up data collection v2 (2020) confined to Match-up pairs in specific ground temperature sensor depths (0.75, 1, 2 m). In situ data in discrete depths of 0.75, 1, 2 m, and Permafrost_cci MAGT SIN is given in ranges with steps of 1 °C. Excluded are sites which are anomalies on the landscape scale, sites in high mountain areas and on arctic mountain tops, and sites within Siberian Yedoma (shape file from Bryant et al., 2017).

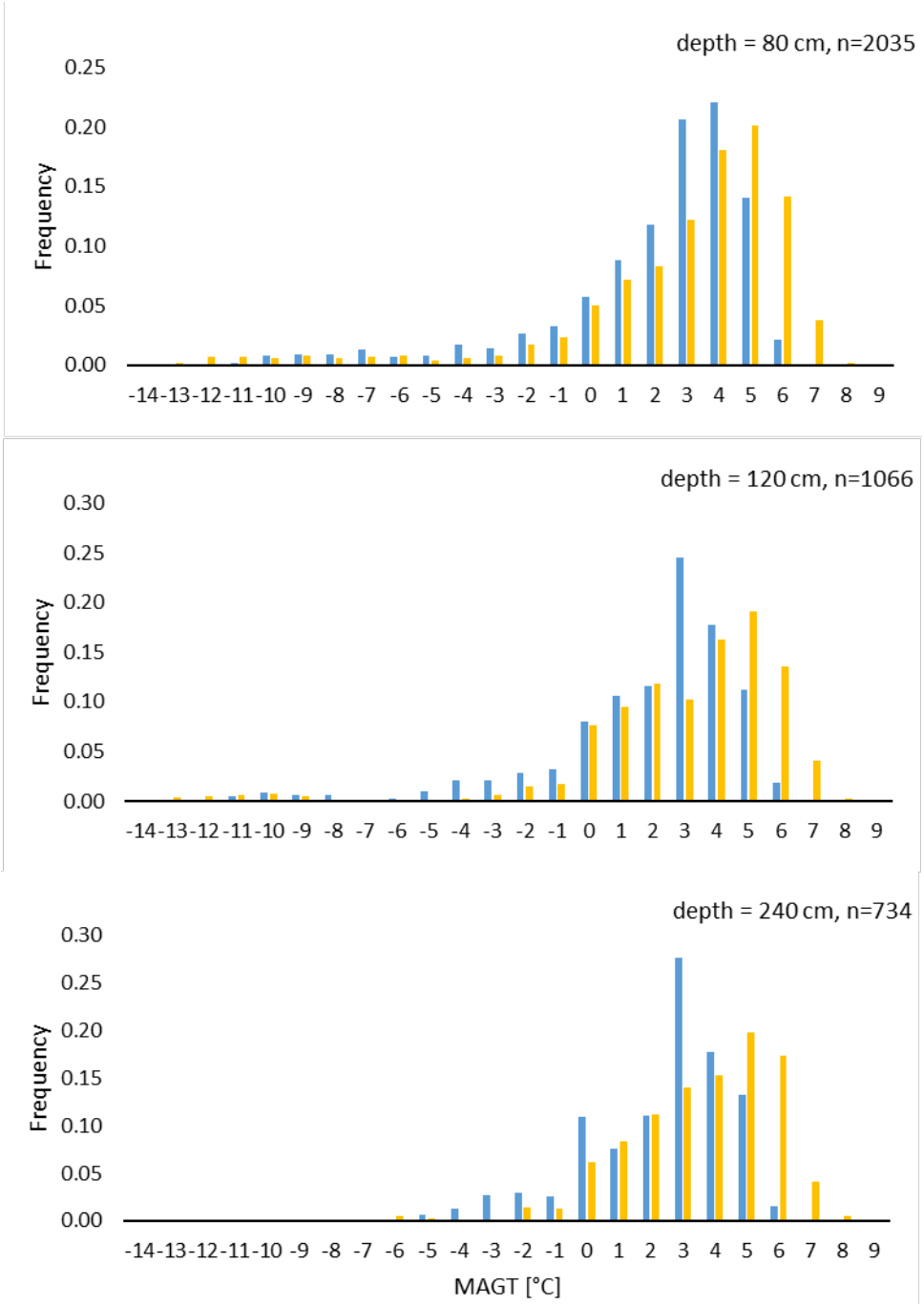

Figure 2.9. Frequency distribution of the Match-up data collection v2 (2020) confined to Match-up pairs in specific ground temperature sensor depths (0.80, 1.20, 2.40 m). In situ data in discrete depths of 0.80, 1.20, 2.40 m, and Permafrost_cci MAGT SIN is given in ranges with steps of 1 °C. Excluded are sites which are anomalies on the landscape scale, sites in high mountain areas and on arctic mountain tops, and sites within Siberian Yedoma (shape file from Bryant et al., 2017).

2.2.3 PERMOS Reference GST and GTD data generation

The PERMOS network currently comprises 27 boreholes distributed within 16 sites (Figure 2.13) across Switzerland, which continuously measure permafrost temperatures between 0 and 100 m depth. The sites are located at elevations between 1580 m a.s.l. and 3400 m a.s.l. with boreholes drilled in bedrock, rock glaciers, talus slopes, steep rock walls or moraines ([RD-5], Table 4.4).

For each single borehole, PERMOS selected the thermistor closest to the depth of the Permafrost_cci GTD POL product (0, 1, 2, 5 and 10 m) and compiled mean annual ground temperature (MAGT) over the period 1997-2018. Only data series with at least 80% data completeness over the year were selected for computing MAGT.

The Match-up of the 1 km x 1 km grid cell of the Permafrost_cci product with the in situ data functions by selecting the grid cells in which the boreholes are located. The in situ measured and Permafrost_cci simulated MAGT values are compared pairwise for each single borehole and depth. In mountainous terrains, the differences in the subsurface thermal regime due to varying climate conditions are considered smaller than those caused by topography or surface and subsurface conditions of the different landforms. Therefore, we analysed the model performance based on the landform typologies rather than based on climatic regions.

Ground surface temperature (GST) are temperatures measured between 0 and 10 cm depth by miniature loggers placed only with a small distance below the surface to avoid the influence of the direct shortwave radiation and to capture a slightly filtered temperature signal. Within the PERMOS network, GST are measured at 23 different sites, each with 4 to more than 20 individual loggers adding up to 247 measurement points (see also Figure 2.13). Each logger measures continuously with a temporal resolution of 1 to 3 hours.

Based on this data set, PERMOS computed mean annual ground surface temperature (MAGST) for each single logger over the period 1997 to 2018. Only series with at least 80% data completeness over the year were selected for computing the annual mean. Thus, the number of MAGST available is variable from one year to the next. It ranges from 16 MAGST match-up data computed in 1997 to 242 in 2011.The MAGST data is highly variable depending on snow conditions, radiation and shading effects as well as surface and subsurface properties. The variability within one specific site (i.e., 4 to 30 loggers) is thus in the same range as the variability in-between the different sites.

Given the high impact of topography and other (sub-)surface properties on the GST, a direct Match-up between the 1 km x 1 km grid cell of the Permafrost_cci GTD product and single point locations is inapplicable. Therefore, we computed the average MAGST of all available GST logger and compared it to the average of all Permafrost_cci GT POL grid cells located between 2000 and 3000 m a.s.l.

2.2.4 Satellite derived Freeze/Thaw Surface Status GT evaluation data set generation

The Freeze-Thaw to Temperature (FT2T) model is an empirical model, based on a linear regression analysis between the annual sum of frozen days, measured with microwave EO sensors, and in-situ ground temperature measurements (Kroisleitner et al., 2018). It was initially developed for temperature retrieval at coldest sensor depth spanning the years 2007-2013 avaiable from Paulik et al. 82014). The method by Naeimi et al. (2012) which forms the basis for the 2007-2013 record of Paulik et al. (2014) has been applied to further records, extending the dataset to 2018. The method and set parameters were evaluated by in situ records and C-band SAR data (Sentinel-1; Bergstedt et al. 2020b). A Metop ASCAT global gridded data set available from EUMETSAT (SOMO12) has been used for this purpose. FT2T has been further developed for Permafrost_cci to represent the depths of the CRDPv1 and calendar years. With respect to in situ data availability for the model calibration, only depths of 1 m, 5 m and 10 m can been considered. Further improvements have been made regarding bias correction for lake fraction using Sentinel-1 (Bergstedt et al., 2020a). These apply to lake rich regions. Records have been extracted for selected borehole locations of the match-up data set for site comparisons in addition to the circumpolar comparison presented in [RD-7].

2.3 Assessment of Active Layer Thickness

2.3.1 In-Situ Active Layer Thickness Reference Data Generation

The comprehensive CALM data collection of ALT time series is available for download on https://www2.gwu.edu/~calm/. For an estimation of ALT, it is relevant to measure active layer depths in the end of the active-layer thawing season. This maximum thaw depth measured in late summer represents the ALT of a specific year. For some measurements in the CALM ALT data collection, metadata information indicate that a value was measured earlier in summer during a year. These active layer depth measurements, not representing the Permafrost ECV ALT, were discarded.

Version 1 synthesised active layer thickness match-up collection (2003 to 2017) (2019)

Permafrost_cci Match-up data set in phase 1, Version 1: standardised active layer thickness ALT data with annual resolution from 2003 and 2017 with a circum-Arctic geographic coverage. The collection contained data from 207 sites (China + Mongolia: 67, Greenland + Svalbard + Scandes: 11, Canada: 6, Russia: 57, USA: 207), with overall 1835 match-up pairs in time.

Version 2 synthesised active layer thickness match-up collection (1997 to 2018) (2020)

Permafrost_cci Match-up data set in phase 2, Version 2: standardised active layer thickness ALT data with annual resolution from 1997 and 2018 with a circum-Arctic geographic coverage. The collection contains data from 156 sites with 1835 Match-up pairs. Please note that we excluded all sites in Mongolia, Central Asia, and on the Tibetan Plateau.
Please also note that we excluded in the 2020 validation also all sites within the Siberian Yedoma area (Bryant et al., 2017) due to incorrect parameterisation of Permafrost_cci CryoGrid of Yedoma stratigraphy

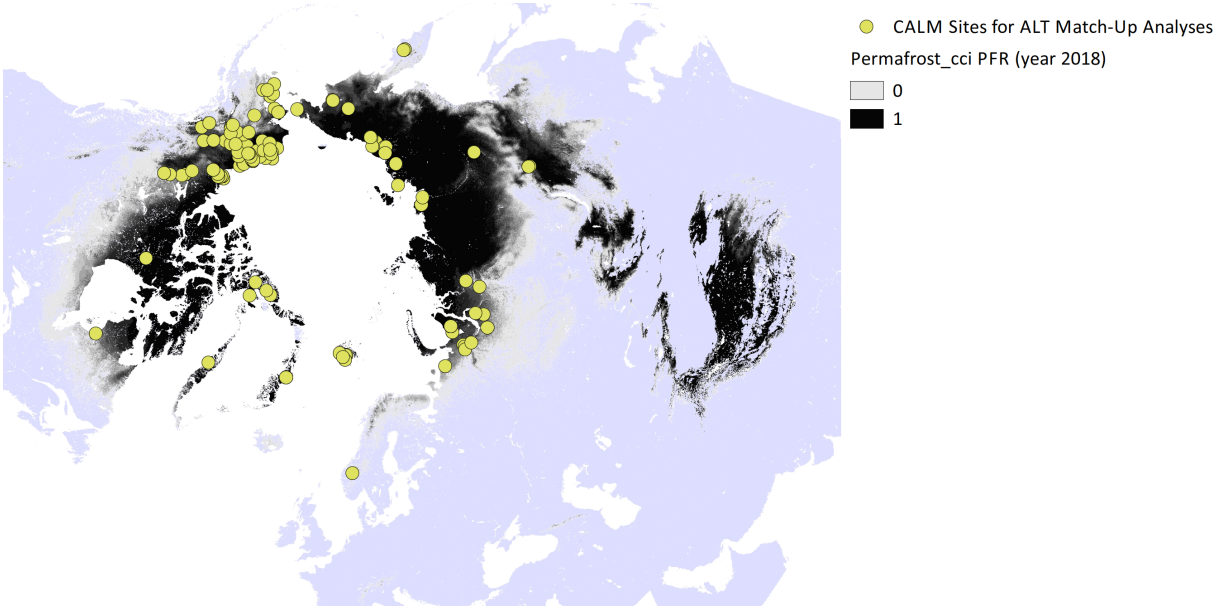

Figure 2.10. Northern hemisphere Permafrost_cci PFR permafrost probability and in situ sites of active layer depth ALT (GTN-P CALM programme).

2.3.2 Characteristics of ALT match-up data set

ALT can, by definition, only occur within permafrost. Therefore, the characteristics of the ALT Permafrost_cci and ALT in situ data collections represent all data sampled in permafrost zones.

The frequency distribution of the ALT Match-up data set shows the data set characteristics of

i) in situ data collection GTN-P CALM ALT
ii) CRDPv1 Permafrost_cci ALT SIN and POL

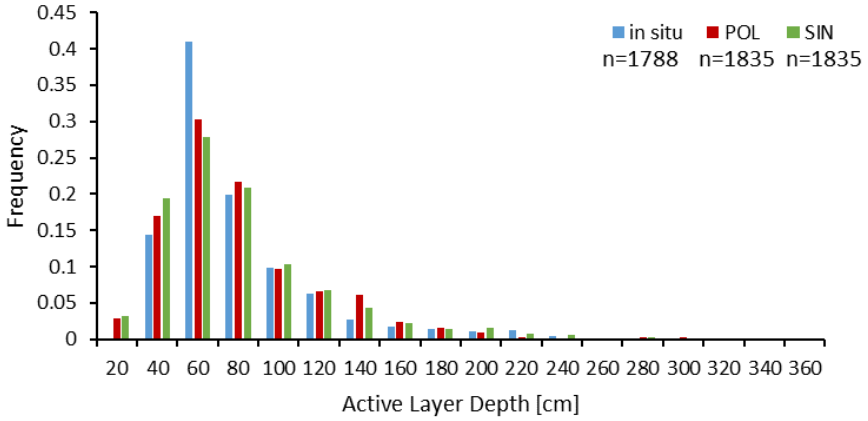

Figure 2.11. Frequency distribution of Permafrost_cci ALT POL and SIN and in situ ALT from GTN-P CALM.

The characteristics of Permafrost_cci ALT POL and SIN show a unimodal right-skewed distribution with a maximum around 40-80 cm depth, similar to in situ CALM ALT (Figure 2.11). However, Permafrost_cci ALT POL and SIN show an overrepresentation of shallow ALT values in the range of 0-20 cm and an underrepresentation at 60 cm, which is the most abundant class in the CALM ALT in situ data set (see Figure 2.11).

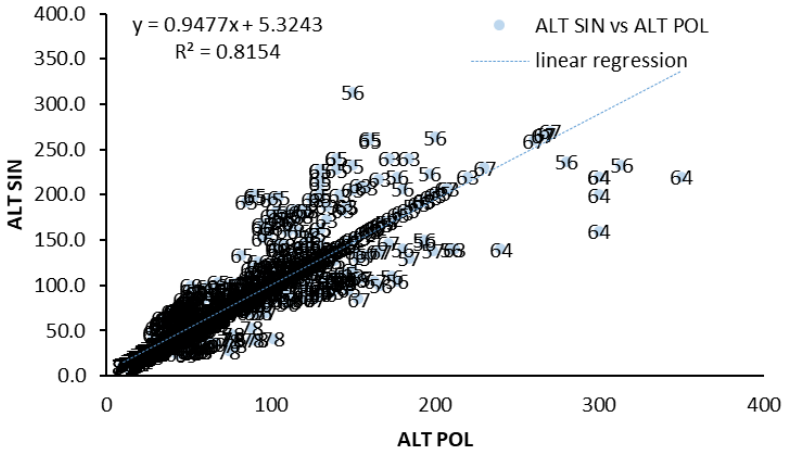

Figure 2.12. Comparison of Permafrost_cci ALT POL vs Permafrost_cci ALT SIN at Match-up sites. ALT in cm, labels show latitudes.

Permafrost_cci ALT POL is, in general, similar to Permafrost_cci ALT SIN, with a linear fit intercept of 5 cm and a linear fit slope of 0.95 (Figure 2.12). However, it appears there are several measurement locations, due to spatial heterogeneity, where the grid cell shift and the higher averaging of the Permafrost_cci POL in contrast to the Permafrost_cci SIN product becomes obvious in a high over- and underestimation, respectively. This data set characteristic of Permafrost_cci MAGT POL (that it contains less spatial details and appears more averaged at the landscape scale) seems to become even more prominent in the southern permafrost zones at lower latitudes.

2.4 Assessments of Permafrost Extent

2.4.1 In Situ PE Reference Data Generation

Match-up Version 1 synthesised binary Permafrost Extent PFR (CRDPv0 2019)

Match-up data set in phase 1, Version 1:

- Permafrost_cci CryoGrid-3 Permafrost fraction PFR per site and year given in 0, 20, 40, 60, 80 or 100%
- A binary PFR data set from 2003 to 2017 was compiled from Version 1 synthesised mean annual GTD - discrete depths.
- Criteria permafrost abundance yes / no
- One data set with Yes all measurements in depths (0 – 2m) MAGT ≤0.5 °C

Match-up Version 2 synthesised binary Permafrost Extent PFR (CRDPv1 2020)

Match-up data set in phase 2, Version 2:

- Permafrost_cci CryoGrid 3 Permafrost fraction PFR per site and year is given in 0, 14, 29, 43, 57, 71 or 100%
- A binary PFR data set from 1997 to 2018 is compiled from Version 2 synthesised mean annual GTD - discrete depths and Version 2 synthesised annual CALM ALT and active layer depth measurements from Russian expeditions (Bartsch, oral communication, 2020)
- Criteria permafrost abundance yes / no
- One data set with Yes if any measurements in depths (0 – 2.4 m) MAGT ≤0.5 °C and Yes to all ALT and ALD measurements <300 cm
- Accuracy = (TP+TN)/(TP+TN+FP+FN),
  where: TP = True positive; FP = False positive; TN = True negative; FN = False negative
- The formula for quantifying binary precision is: Precision = (TP) / (TP+FP)

2.4.3 PERMOS Reference PFR Data Generation

The best visual expression of mountain permafrost is represented by rock glaciers, which, in contrast to the sub-ground permafrost itself, can be mapped and monitored directly using remotely sensed data. Rock glaciers are lava stream-like mixtures of permanently frozen debris that creep downslope under gravity. Their abundance can be used as validation for the high permafrost probability extent.
The information on rock glacier abundance and extent was computed within the GlobPermafrost program and is available since 2017 for the Bas-Valais region (Figure 2.13). From this inventory, PERMOS specifically selected the landforms indicative for permafrost occurrence (i.e., rock glaciers, push-moraines and complex landforms including both rock glaciers and push-moraines) and compared the Permafrost_cci PFR POL product with this inventory of permafrost landforms.

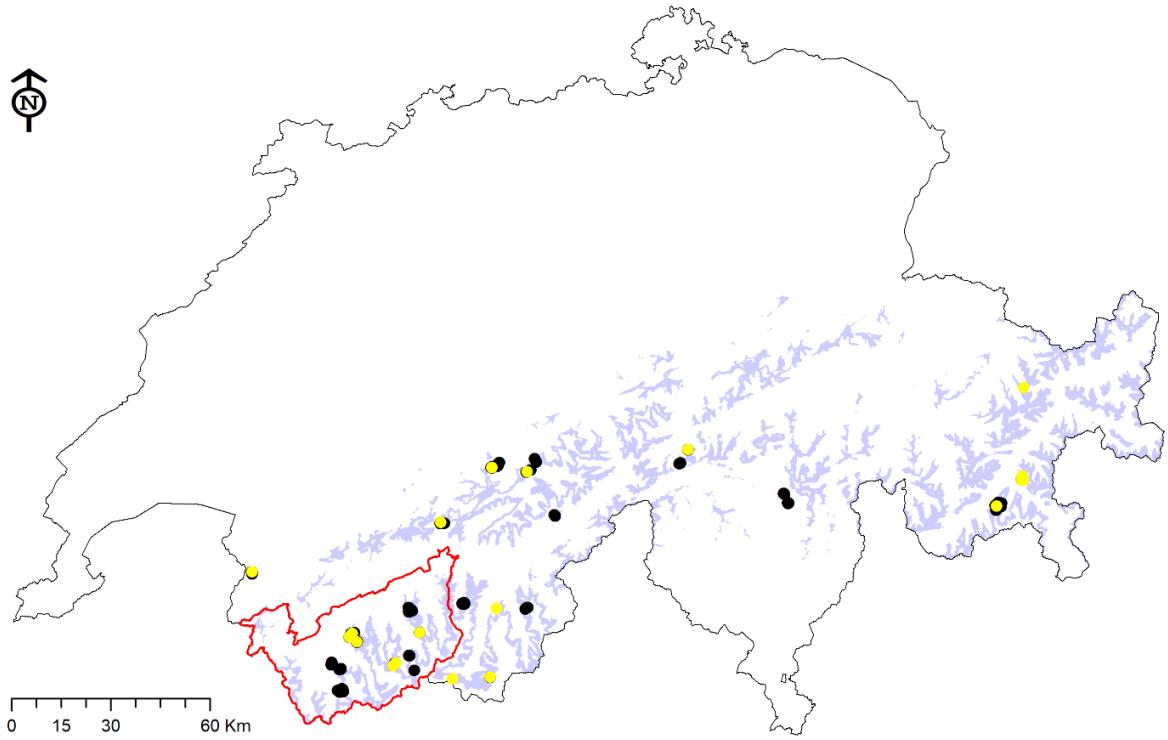

Figure 2.13. Location of the 247 GST logger (black circles), 28 GT boreholes (yellow circles) and the extent of the ESA GlobPermafrost rock glacier inventory (red outline) used for the validation of the Permafrost_cci GTD product in the Swiss Alps. The bluish colour-coded zones represent the areas located between 2500 m and 3000 m a.s.l.

3 ASSESSMENT RESULTS: PERMAFROST TEMPERATURE

3.1 Permafrost Temperature User Requirements

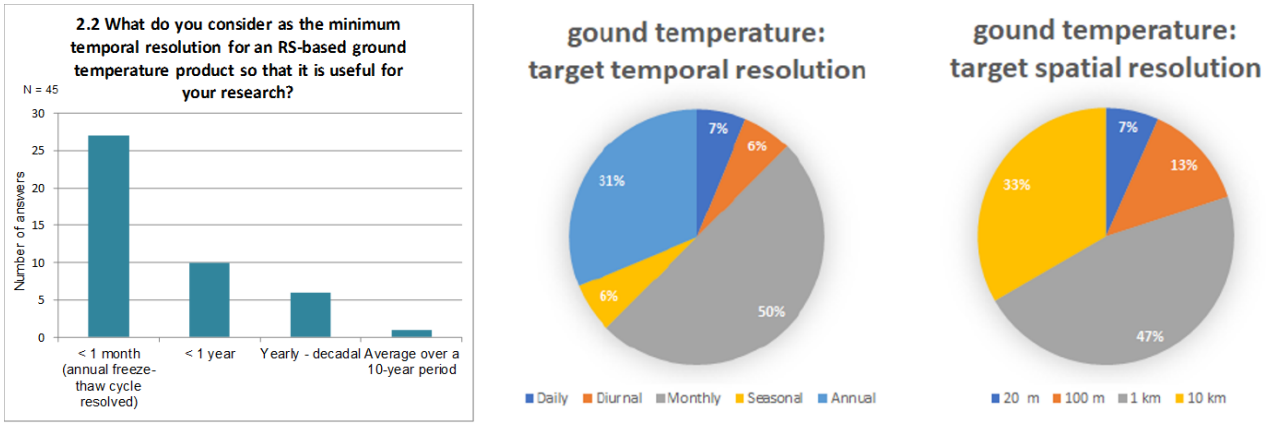

Figure 3.1a,b. User Survey results. Left: ESA DUE GlobPermafrost User Survey results, question 2.2 [RD-1]. Right: ESA CCI Permafrost User Survey results, Figure 3 [RD-4].

Users of potential products of permafrost temperature are interested in high temporal resolution: monthly or higher as documented in [RD-1, RD-2, RD-4]. However, 30% of users also rated annual resolution as adequate as target temporal resolution in [RD-4]. Half of the user group are satisfied with a target spatial resolution of 1 km. The first release of the Permafrost_cci CRDPv0 MAGT provided annual resolution with 1×1 km spatial resolution over a range of depths (0, 1, 2, 5, 10 m) from 2003 to 2017, the 2nd release Permafrost_cci CRDPv1 MAGT provides annual resolution with 1×1 km resolution over the same range of depths (0, 1, 2, 5, 10 m) but covering a longer time span from 1997 to 2018.

3.2 Permafrost_cci MAGT Match-Up Analyses with In Situ Data

The Match-up is performed for Permafrost_cci MAGT versus in situ MAGT for i) the complete MAGT data collection and ii) confined to permafrost temperature only (that we restrict to in situ MAGT <1 °C). For each in situ point location, the pixel value in the Permafrost_cci SIN and POL products closest to the in situ measurement was extracted to produce the Match-up data set and derive statistics.

The first Match-up analyses is performed with all depths using Permafrost_cci SIN MAGT.

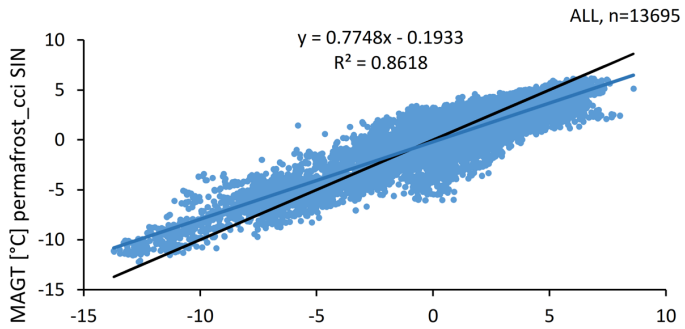

	MAGT SIN mean bulk
bias	-0.53
abs_bias	1.33
RSME	1.65
slope	0.77
intercept	-0.19
r^2	0.86

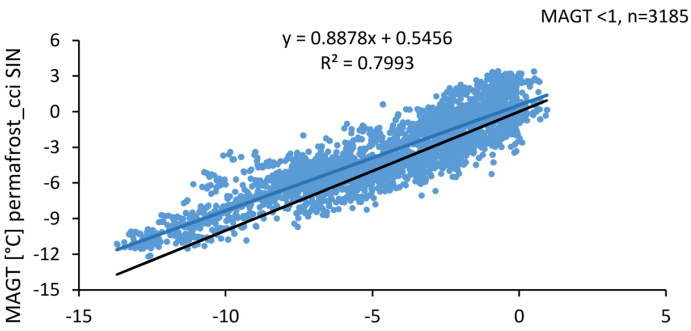

	MAGT SIN mean MAGT <1 °C
bias	1.05
abs_bias	1.54
RSME	1.85
slope	0.89
intercept	0.55
r^2	0.80

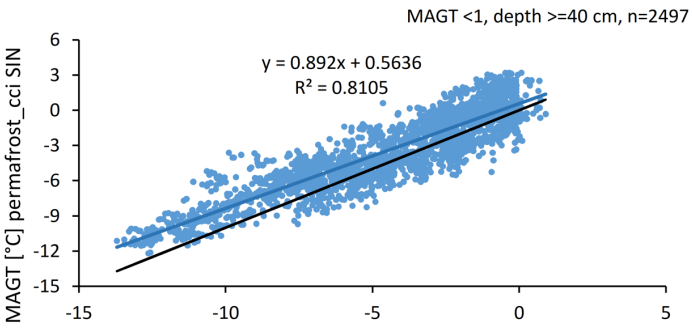

	MAGT SIN mean MAGT <1 °C depth ≥40 cm
bias	1.04
abs_bias	1.52
RSME	1.82
slope	0.89
intercept	0.56
r^2	0.81

Figure 3.2. Regression of Permafrost_cci MAGT SIN versus in situ MAGT in all discrete depths for different data subsets. Statistics of Permafrost_cci MAGT SIN versus in situ MAGT in all discrete depths are given for the respective subsets.

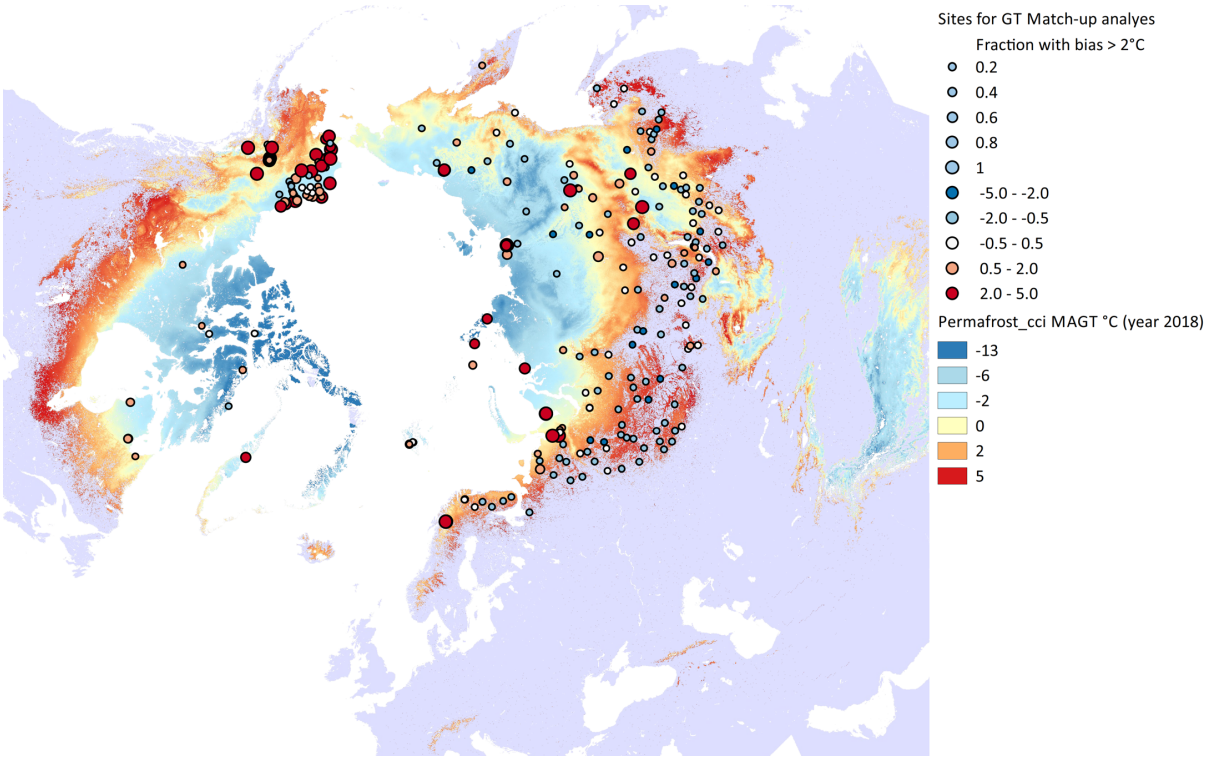

Figure 3.3. Sites included in the Permafrost_cci MAGT match-up analyses. Point-size depicts fractions of values over all depths and years per site with a bias <-2 °C or >2 °C, colours represent the product-bias over all years and depth available. The Background map is the Permafrost_cci GTD in 2 m depth of the year 2018.

Table 3.1. Relative percentage error (RPE) and absolute percentage error (APE) for Permafrost_cci MAGT SIN vs. in situ MAGT per year and depth.

	RPE % SIN	RPE_{5-95} % SIN	APE % SIN	APE_{5-95} % SIN
RPE/APE mean	-35.53	-16.32	166.62	51.30
RPE/APE SD	2441.72	46.93	2436.29	57.84
5% Quantile	-185.80		3.78	
95% Quantile	142.77		378.65	
Precision (SD in [-100:100] range)	35.71		22.04	

Table 3.2. Relative percentage error (RPE) and absolute percentage error (APE) for Permafrost_cci MAGT SIN vs. in situ MAGT per year and depth per latitudinal range.

Latitude (°)	RPE % SIN	RPE_{5-95} % SIN	APE % SIN	APE_{5-95} % SIN
48				
50	-14.41	-14.41	20.39	22.36
52	**-115.57**	-21.54	**180.27**	49.05
54	-6.12	-35.04	87.80	58.97
56	-67.66	-11.97	81.32	34.33
58	-17.23	-8.30	53.17	35.07
60	17.53	-16.47	79.25	47.94
62	-31.35	-27.08	91.57	58.38
64	**-141.84**	-32.27	**559.27**	61.03
66	67.89	-21.96	**281.15**	67.60
68	**-143.47**	-20.77	**346.82**	77.29
70	9.42	2.69	53.90	48.44
72	22.16	22.16	25.71	26.44
74	17.17	17.17	18.14	20.69
78	16.06	16.06	16.50	18.32
80	21.44	22.17	33.74	35.24

Table 3.3. MAGT bias (mean difference of Permafrost_cci MAGT and in situ MAGT) and RMSE (root mean square error) per depth data group for Permafrost_cci MAGT SIN.

	bias	abs_bias	RMSE	n
depth (cm)	v_2	v_2	v_2	v_2
0	1.20	1.60	0.01	59
20	-0.44	1.09	1.43	2100
25	1.13	1.63	1.98	419
40	-0.55	1.12	1.44	2091
50	1.18	1.63	1.98	436
60	0.64	1.37	1.52	13
75	1.06	1.54	1.85	346
80	-0.86	1.28	1.57	2035
100	1.28	1.56	1.86	245
120	-1.07	1.35	1.65	1066
160	-1.21	1.45	1.74	1951
200	1.31	1.48	1.74	107
240	-1.29	1.42	1.68	734
250	0.87	1.11	1.26	33
300	1.26	1.47	1.71	201
320	-1.32	1.51	1.79	1368
400	1.39	1.51	1.76	85
500	1.39	1.58	1.86	209
1000	1.28	1.46	1.70	197
mean	**0.38**	**1.43**	**1.61**	**∑ 13695**

Table 3.4. Regression-parameters for x=in situ MAGT, y= Permafrost_cci MAGT SIN - slope of the best linear fit equation (S), intercept of the best linear fit equation (I), coefficient of correlation (r), number of measurements (n).

	S	I	r^2	n
0	0.8146	0.0484	0.8154	59
20	0.8214	-0.0323	0.8655	2100
25	0.8781	0.6240	0.7102	419
40	0.8166	-0.1315	0.8768	2091
50	0.9082	0.8143	0.7221	436
60	0.6330	-1.6962	0.8388	13
75	0.9536	0.8567	0.7314	346
80	0.8226	-0.4362	0.8684	2035
100	0.9406	1.0137	0.8140	245
120	0.8399	-0.6788	0.8583	1066
160	0.8550	-0.7909	0.7950	1951
200	0.9736	1.2013	0.9054	107
240	0.8853	-0.9325	0.7821	734
250	0.2642	-0.8516	0.0986	33
300	0.8691	0.8412	0.8961	201
320	0.7987	-0.6551	0.7250	1368
400	0.9431	1.2017	0.8440	85
500	0.7852	0.7605	0.8810	209
1000	0.8128	0.7271	0.8976	197

Match-up comparison to the MAGT SIN depth time series collection (1997 to 2018) of all depths and the full temperature range, n = 13695

Permafrost_cci MAGT SIN performance for warm (non-permafrost) and cold (permafrost) temperature groups in situ MAGT is characterised by:

- an absolute bias of ~ 1.33 °C if calculated pairwise in the bulk data set, an absolute bias of 1.43 °C if calculated in depth-specific data collections.
- RMSE of 1.65 °C if calculated pairwise in the bulk data set, and RMSE of 1.61 °C if calculated in depth-specific data collections.
- a relative percentage error of -17% (within the 5 to 95% Quantile), absolute percentage error ~52% (within the 5 to 95% Quantile).

Assessment of Permafrost Temperature (MAGT <1 °C)

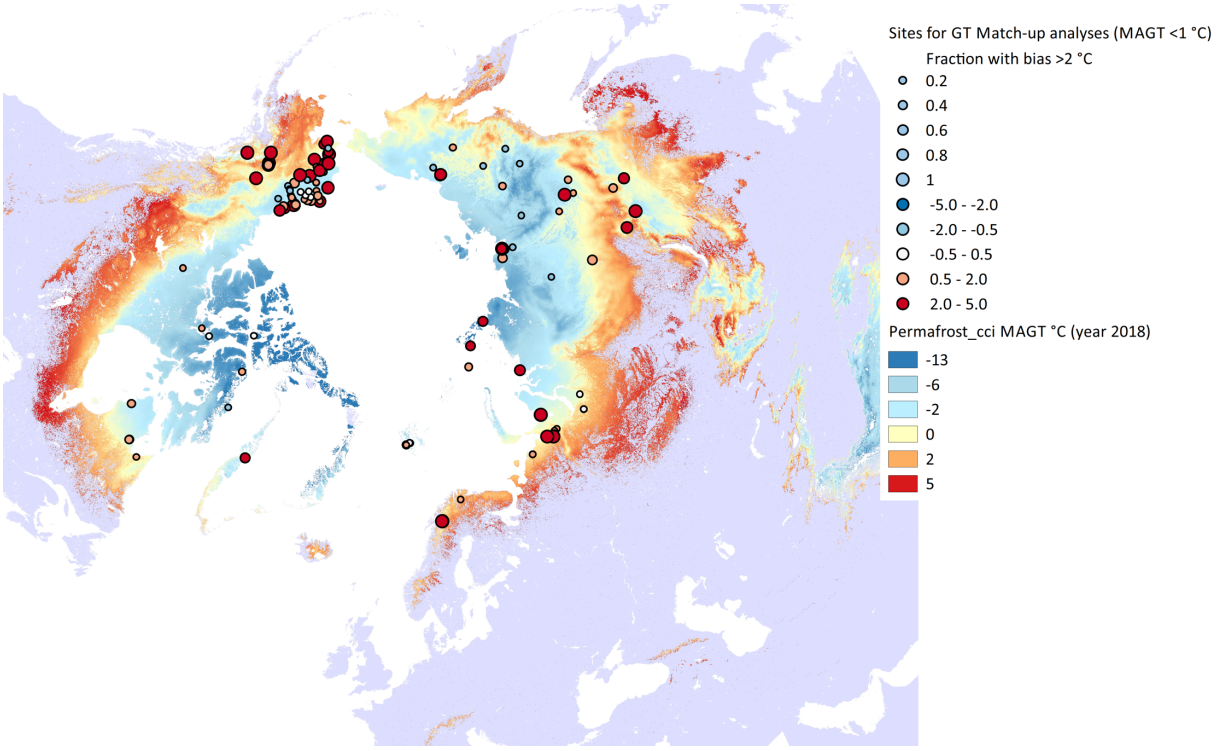

Figure 3.4. Sites included in the Permafrost_cci MAGT Match-up analyses for sites with MAGT ≥1 °C discarded. Point-size depicts fractions of values over all depths and years per site with a bias <-2 °C or >2 °C, colours represent the product-bias over all years and depth available.. The Background map is the Permafrost_cci GTD in 2 m depth of the year 2018.

Table 3.5. MAGT bias (mean difference of Permafrost_cci MAGT and in situ MAGT) and RMSE (root mean square error) per Latitude for Permafrost_cci MAGT SIN. Sites with MAGT≥1°C discarded.

	bias	abs_bias	RMSE	n
Latitude (°)	v_2	v_2	v_2	v_2
54				
56	2.36	2.36	0.74	11
58	0.66	0.96	0.14	96
60	2.00	2.01	0.16	193
62	0.66	1.23	0.12	156
64	0.54	1.58	0.15	177
66	1.32	1.76	0.12	315
68	1.11	1.50	0.12	224
70	0.31	1.29	0.05	909
72	1.80	1.95	0.10	511
74	1.46	1.54	0.12	254
78	1.78	1.83	0.28	53
80	1.23	1.36	0.09	287

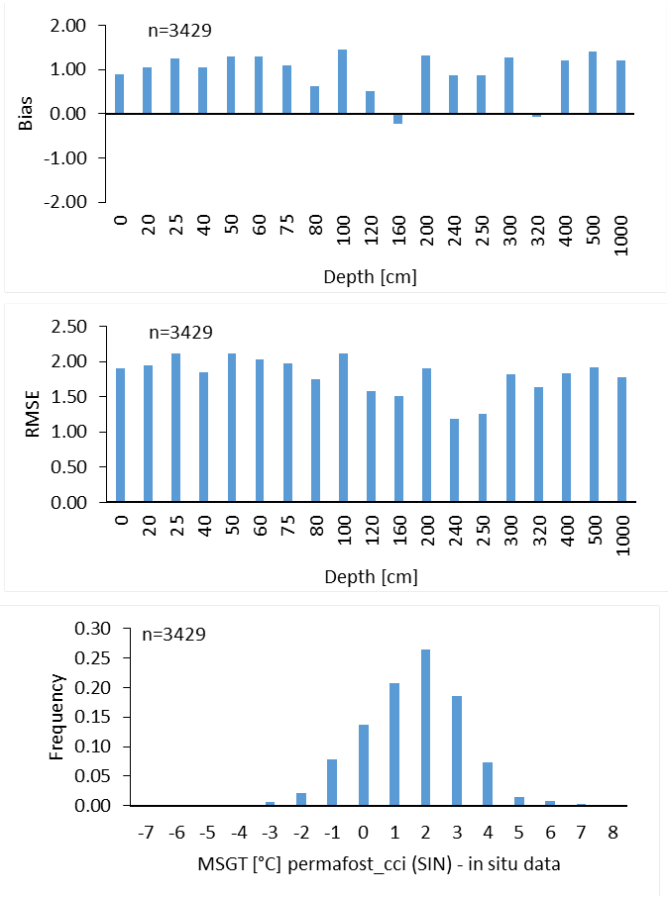

Figure 3.5. Characteristics of the MAGT Match-up data collection v2 (2020), with sites with in situ MAGT ≥1 °C excluded, n = 3186 per depth and per bias magnitude. Upper graph shows MAGT bias (in °C) (mean difference of Permafrost_cci MAGT minus in situ MAGT) and the central graph shows MAGT RMSE (in °C) (root mean square error) for Permafrost_cci MAGT SIN visualised in the most frequent temperature sensor measurement depths. The lower graph shows the frequency distribution of the magnitude of the MAGT bias.

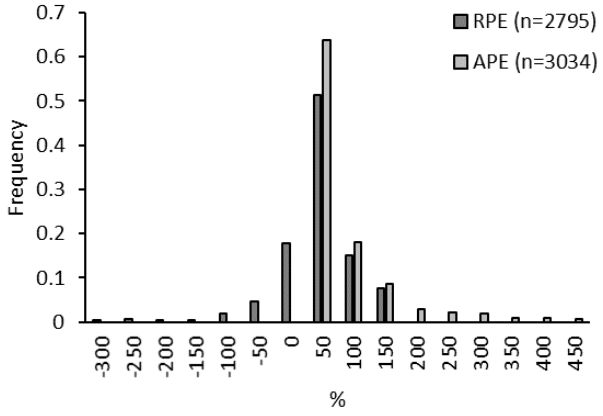

Figure 3.6. Frequency distribution of the MAGT Match-up data collection v2 (2020), with sites with in situ MAGT ≥1 °C excluded, n = 3186 of relative percentage error RPE and absolute percentage error APE of Permafrost_cci MAGT SIN (within the 5-95% Quantile range);

Table 3.6. Regression-parameters of the MAGT Match-up data collection v2 (2020), with sites with in situ MAGT ≥1 °C excluded, n = 3186 for x=in situ MAGT, y= Permafrost_cci MAGT SIN - slope of the best linear fit equation (S), intercept of the best linear fit equation (I), coefficient of correlation (r), number of measurements (n).

depth (cm)	S	I	r²	n
0	0.8423	0.2614	0.7946	57
20	0.8744	0.3173	0.8151	251
25	0.8494	0.4740	0.6259	381
40	0.8720	0.3011	0.8371	249
50	0.8842	0.6720	0.6432	394
60	0.6330	-1.6962	0.8388	13
75	0.9178	0.6438	0.6534	318
80	0.8169	-0.4266	0.8329	224
100	0.9551	1.0887	0.7443	214
120	0.7896	-0.8347	0.9198	69
160	0.9793	0.3003	0.8312	134
200	0.9998	1.3638	0.9113	104
240	1.2776	2.4566	0.8671	7
250	0.2642	-0.8516	0.0986	33
300	0.8740	0.8713	0.8975	199
320	1.1549	0.2543	0.7658	60
400	0.9623	1.2890	0.8390	83
500	0.7971	0.8307	0.8845	203
1000	0.8198	0.7685	0.8990	193

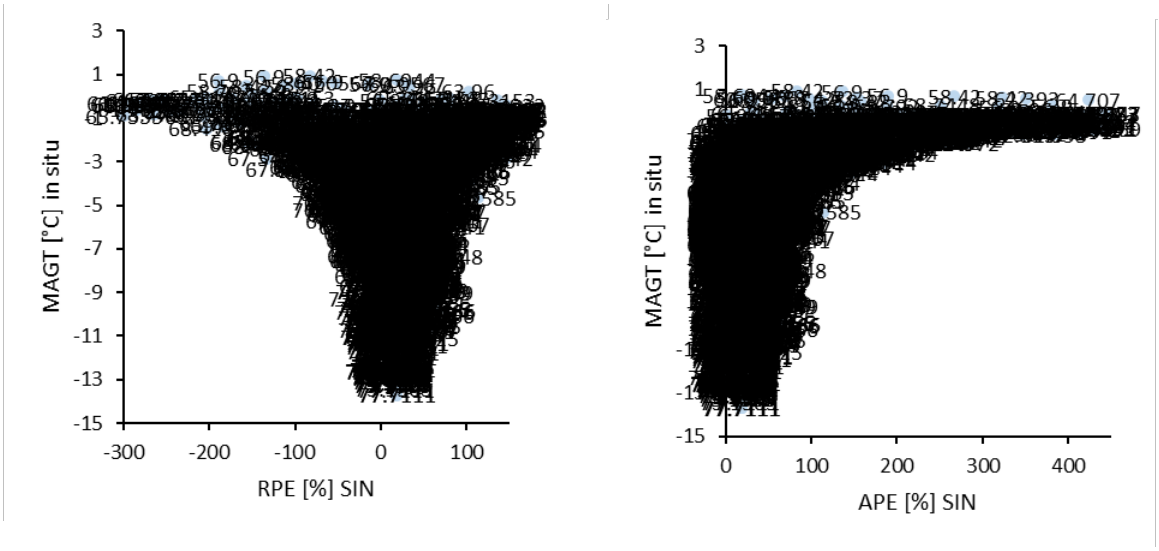

Figure 3.7. MAGT Match-up data collection v2 (2020), with sites with in situ MAGT ≥1 °C excluded, n = 3186. Relative percentage error RPE and absolute percentage error APE of match up synthesised in situ MAGT at all discrete depths and Permafrost_cci MAGT SIN versus in situ MAGT). Labels = Latitude.

Table 3.7. MAGT Match-up data collection v2 (2020), with sites with in situ MAGT ≥1 °C excluded, n = 3186. Relative percentage error (RPE) and absolute percentage error (APE) for Permafrost_cci MAGT SIN vs. in situ MAGT per year and depth.

	RPE % SIN	RPE_{5-95} % SIN	APE % SIN	APE_{5-95} % SIN
RPE/APE mean	106.76	37.97	193.73	63.83
RPE/APE SD	3508.43	65.10	3504.70	75.26
5% Quantile	-97.12		3.45	
95% Quantile	328.42		430.09	
Precision (SD in [-100:100] range)	36.49		24.51	

Table 3.8. MAGT Match-up data collection v2 (2020), with sites with in situ MAGT ≥1 °C excluded, n = 3186. Relative percentage error (RPE) and absolute percentage error (APE) for Permafrost_cci MAGT SIN vs. in situ MAGT per year and depth per latitudinal range.

Latitude (°)	RPE % SIN	RPE_{5-95} % SIN	APE % SIN	APE_{5-95} % SIN
54				
56	106.46	106.46	106.46	106.46
58	44.08	51.17	134.71	99.98
60	260.72	129.02	269.09	139.15
62	-61.64	39.99	126.33	95.50
64	1326.24	14.27	1346.90	61.36
66	16.81	113.12	593.26	148.65
68	99.21	87.81	119.80	104.57
70	9.97	13.29	56.17	51.09
72	22.16	22.41	25.71	26.40
74	17.17	17.17	18.14	20.39
78	16.06	16.06	16.50	17.72
80	21.44	25.47	33.74	35.01

Table 3.9. MAGT Match-up data collection v2 (2020), with sites with in situ MAGT ≥1 °C excluded, n = 3186. MAGT bias (mean difference of Permafrost_cci MAGT and in situ MAGT) and RMSE (root mean square error) per depth data group for Permafrost_cci MAGT SIN.

	bias		abs_bias	RMSE		n	
depth (cm)	v_2	v_1	v_2	v_2	v_1	v_2	v_1
0	1.29	-2.61	1.62	1.94	3.04	57	42
20	1.04	-2.19	1.59	1.95	3.35	251	185
25	1.15	-1.4	1.67	2.02	2.31	381	399
40	1.06	-1.32	1.51	1.86	2.37	249	190
50	1.19	-0.67	1.67	2.02	1.86	394	407
60	0.64	-1.14	1.37	1.52	1.9	13	18
75	1.03	-0.27	1.55	1.87	1.59	318	304
80	0.61	-0.4	1.42	1.76	2.04	224	161
100	1.32	0.67	1.60	1.90	1.64	214	208
120	0.52	-0.21	1.35	1.58	2.44	69	44
160	-0.23	-0.44	1.26	1.51	2.06	134	87
200	1.36	1.05	1.50	1.75	1.64	104	103
240	0.86	-0.46	0.86	1.19	0.83	7	6
250	0.87	0.41	1.11	1.26	1.12	33	33
300	1.28	0.65	1.47	1.72	1.28	199	191
320	-0.08	-0.69	1.46	1.64	1.99	60	46
400	1.42	0.69	1.54	1.78	1.33	83	69
500	1.45	0.34	1.61	1.88	1.16	203	179
1000	1.32	0.12	1.48	1.71	1.06	193	169
			1.62				
mean	**0.95**	**-0.41**	**1.45**	**1.73**	**1.84**	**∑3186**	**∑2841**

Match-up comparison to the MAGT SIN depth time series collection (1997 to 2018) of all depths, MAGT <1 °C, n = 3186

Permafrost_cci MAGT SIN performance for all depths for in situ permafrost MAGT (restricted to MAGT <1 °C) is characterised by:

- a bias of 1.05 °C and an absolute bias of ~1.54 °C if calculated pairwise in the bulk data set, a bias of 0.95 °C and an absolute bias of 1.45 °C if calculated in depth-specific data collections.
- RMSE of 1.85 °C if calculated pairwise in the bulk data set, and RMSE of 1.73 °C if calculated in depth-specific data collections.
- a relative percentage error of 38% (within the 5 to 95% Quantile), absolute percentage error 64% (within the 5 to 95% Quantile).

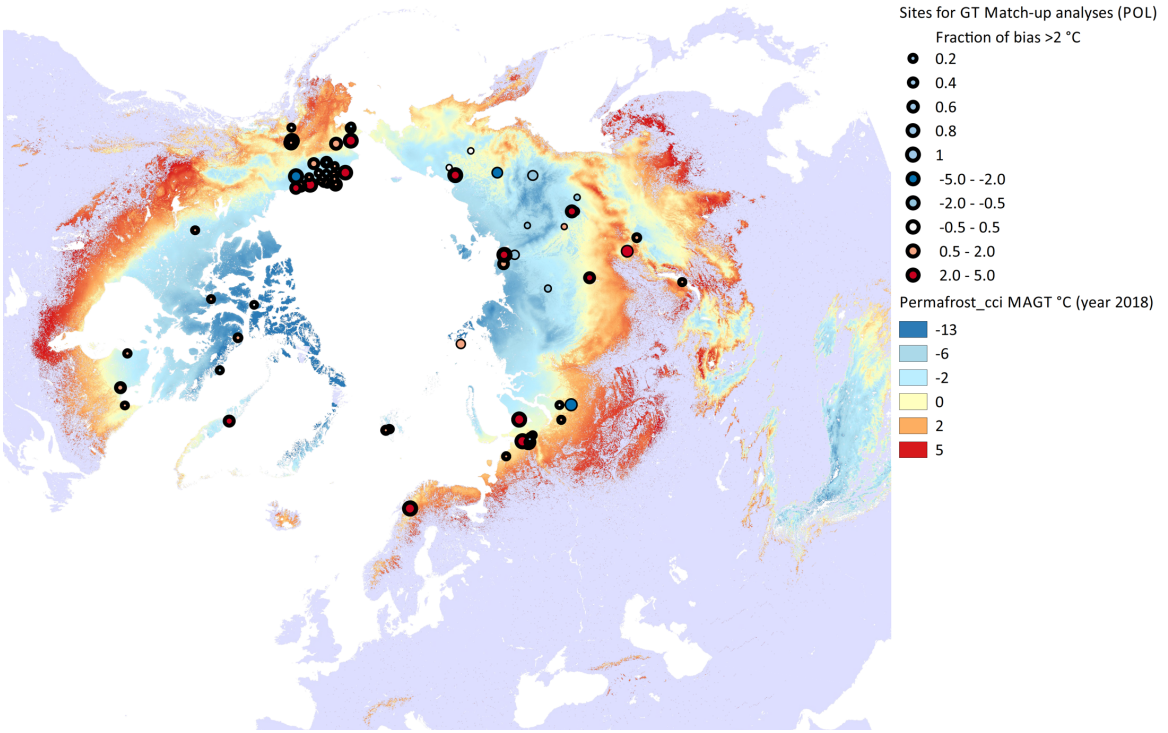

Figure 3.8. Sites included in the Permafrost_cci MAGT POL Match-up analyses. Point-size depicts fractions of values over all depths and years per site with a bias <-2 °C or >2 °C, colours represent the product-bias over all years and depth available. Data from sites with thin outlines are only available via interpolation.

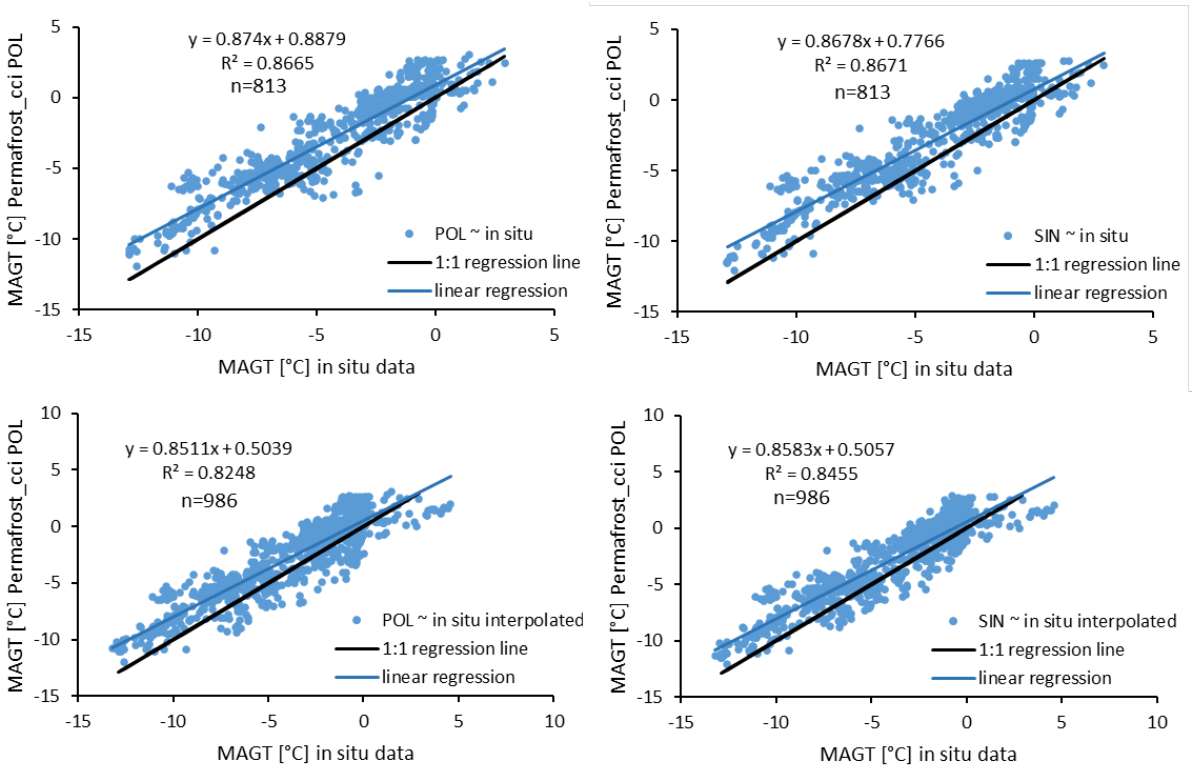

*Figure 3.9. Regression of x=MAGT in situ and y=Permafrost_cci MAGT POL/SIN in 0, 1, 2, 5 and 10 m depth. Data in the lower panel represent **interpolated** values for in situ data.*

Table 3.10. Relative percentage error (RPE) and absolute percentage error (APE) for Permafrost_cci MAGT SIN and for Permafrost_cci MAGT POL and SIN (depths 0, 1, 2, 5, 10 m) of the Match-up versus in situ MAGT (in situ MAGT ≥1 °C excluded) for original in situ data (n=767) and in situ data interpolated between depths (n=924).

	POL				SIN			
	RPE (%)	RPE5-95 (%)	APE (%)	APE5-95 (%)	RPE (%)	RPE5-95 (%)	APE (%)	APE5-95 (%)
mean	91.36	66.16	128.50	85.73	69.35	59.19	107.49	76.93
sd	260.48	69.02	244.30	88.40	212.17	59.30	195.63	71.90
5% Quantile	-64.24		5.98		-79.70		4.65	
95% Quantile	392.66		538.48		266.72		356.93	

interpolated in situ data	POL				SIN			
	RPE (%)	RPE5-95 (%)	APE (%)	APE5-95 (%)	RPE (%)	RPE5-95 (%)	APE (%)	APE5-95 (%)
mean	48.59	52.85	150.99	89.74	48.76	48.97	115.87	76.92
sd	643.86	77.81	627.79	101.58	348.96	65.83	332.75	76.27
5% Quantile	-267.12		5.98		-172.96		3.69	
95% Quantile	384.43		608.09		283.63		373.63	

Table 3.11. Bias, absolute bias and RMSE for Permafrost_cci POL and SIN (depths 0, 1, 2, 5, 10 m) of the Match-up versus in situ MAGT (in situ MAGT ≥1 °C excluded) for original in situ data (n=767) and in situ data interpolated between depths (n=924).

			interpolated	
	POL	SIN	POL	SIN
bias	1.41	1.33	1.14	1.12
abs_bias	1.63	1.54	1.61	1.49
RMSE	1.88	1.81	1.86	1.76

Table 3.12. Bias, absolute bias and RMSE per depth for Permafrost_cci POL and SIN (depths 0, 1, 2, 5, 10 m) of the Match-up versus in situ MAGT (in situ MAGT ≥1 °C excluded) for original in situ data and in situ data interpolated between depths.

					interpolated			
depth (cm)	bias	abs_bias	RMSE	n	bias	abs_bias	RMSE	n
0	1.19	1.62	1.92	61	1.19	1.62	1.90	61
100	1.31	1.63	1.92	206	0.79	1.54	1.71	326
200	1.55	1.67	1.91	104	1.03	1.71	1.69	141
500	1.51	1.67	1.91	203	1.51	1.67	1.88	203
1000	1.42	1.58	1.78	193	1.42	1.58	1.71	193

Match-up comparison to the MAGT POL depth time series collection (1997 to 2018) in 0, 1, 2, 5, 10 m depth, MAGT <1 °C, n = 767 for original and n=924 for interpolated data

Permafrost_cci MAGT POL performance for in situ permafrost MAGT (restricted to MAGT <1 °C) is characterised by:

- a bias of 1.41 and an absolute bias of 1.63 °C if calculated pairwise in the bulk data set,
- RMSE of 1.88 °C if calculated pairwise in the bulk data set
- a relative percentage error of 53% (within the 5 to 95% Quantile), absolute percentage error 90% (within the 5 to 95% Quantile).
- including sites with interpolated in situ MAGT slightly improves the results

The too warm estimates of Permafrost_cci MAGT POL mainly occurs at tundra sites (Alaska and Western Siberia).

Comparison of Match-up v1 and Match up v2 using the POL dataset in 1, 2, 5 and 10 m depth

In summary, Permafrost_cci CRDPv1 (2003 to 2017) shows a less good overall performance than Permafrost_cci CRDPv0 (2003 to 2017) in the depth and time specific match-wise comparison versus in situ MAGT (2003 to 2017). Permafrost_cci CRDPv1 shows warmer MAGT specifically in Arctic regions, e.g. across all tundra sites and, consistently across deeper depths (5 and 10 m depth).

Table 3.13. Relative Percentage error (RPE) and absolute percentage error (APE) for Match-up version v2 (n = 650) and Match-up version v1 (n = 677) of Permafrost_cci MAGT POL CRDPv0 and CRDPv1 (years 2003-2017 and depths of 1, 2, 5 and 10 m). Please note that the values of v1 in the upper table differ from the first report [RD-7] as we adapted the calculation of the RPE by using the absolute in situ MAGT (compare chapter 2.1 of this report). Lower table: calculation of RPE according to procedure of Match-up v1 as comparison.

	CRDPv1/Match-up v2				CRDPv0/Match-up v1			
	RPE (%)	RPE$_{5-95}$ (%)	APE (%)	APE$_{5-95}$ (%)	RPE (%)	RPE$_{5-95}$ (%)	APE (%)	APE$_{5-95}$ (%)
mean	111.73	79.29	138.93	93.53	-22.70	4.98	184.34	81.75
sd	271.09	81.21	258.21	96.05	800.15	94.07	773.92	151.10
5% Quantile	-23.58		7.17		-729.55		3.21	
95% Quantile	529.18		627.00		189.16		968.11	

	CRDPv1/Match-up v2				CRDPv0/Match-up v1			
	RPE (%)	RPE$_{5-95}$ (%)	APE (%)	APE$_{5-95}$ (%)	RPE (%)	RPE$_{5-95}$ (%)	APE (%)	APE$_{5-95}$ (%)
mean	-111.48	-79.08	138.93	93.53	43.33	1.91	184.34	81.75
sd	271.20	81.38	258.21	96.05	800.33	107.87	773.92	151.10
5% Quantile	-529.18		7.17		-150.64		3.21	
95% Quantile	25.61		627.00		758.76		968.11	

Table 3.14. Bias, absolute bias and RMSE per depth for Match-up version v2 (n = 650) and Match-up version v1 (n = 677) of Permafrost_cci MAGT POL CRDPv0 and CRDPv1 (years 2003-2017).

	CRDPv1/Match-up v2				CRDPv0/Match-up v1			
depth (cm)	bias	abs_bias	RMSE	n	bias	abs_bias	RMSE	n
100	1.34	1.68	1.97	184	0.75	1.27	1.61	224
200	1.54	1.67	1.92	99	1.15	1.44	1.73	103
500	1.55	1.66	1.90	188	0.39	0.94	1.19	181
1000	1.47	1.58	1.78	179	0.20	0.85	1.09	169

Table 3.15. Bias, absolute bias and RMSE for Match-up version v2 (n = 650) and Match-up version v1 (n = 677) of Permafrost_cci MAGT POL CRDPv0 and CRDPv1 (years 2003-2017 and depths of 1, 2, 5 and 10 m).

	CRDPv1 Match-up v2	CRDPv0 Match-up v1
bias	1.47	0.58
abs_bias	1.64	1.10
RMSE	1.89	1.41

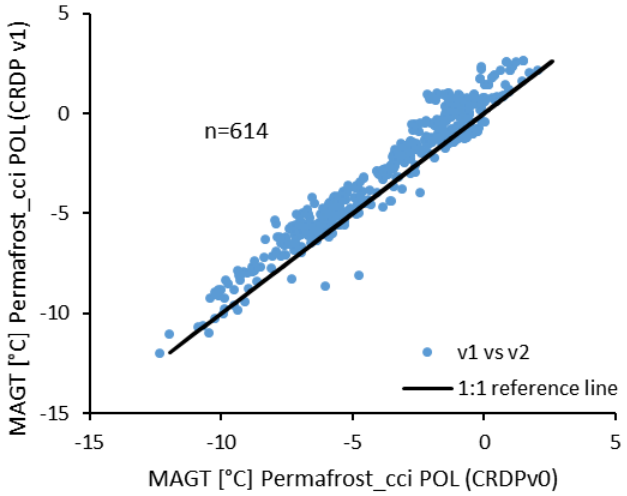

Figure 3.10. Permafrost_cci MAGT POL of CRDPv0 (x-axis) vs Permafrost_cci MAGT POL of CRDPv1 (y-axis).

Match-up comparison to the MAGT POL depth time series collection (2003 to 2017) in 1, 2, 5, 10 m depth, MAGT <1 °C, n = 650

Permafrost_cci MAGT POL performance for in situ permafrost MAGT (restricted to MAGT <1 °C) is characterised by:

- a bias of 1.47 and an absolute bias of 1.64 °C if calculated pairwise in the bulk data set,
- RMSE of 1.89 °C if calculated pairwise in the bulk data set
- a relative percentage error of ~ 80% (within the 5 to 95% Quantile), absolute percentage error 94% (within the 5 to 95% Quantile).

3.3 PERMOS Permafrost Temperature

The comparison of the evolution of the mean in situ measured and modelled MAGST over the Swiss Alps from 1997 to 2018 shows that the model has a warm bias compared to the measurements. However, the warming tendency observed in the measurements is well reproduced by Permafrost_cci GTD POL product (Figure 3.12). The standard deviation of the in situ measurements, although limited to 23 sites, is larger than the variability of the Permafrost_cci GTD product over the entire Swiss Alps. This is emphasized in Figure 3.13 which shows the measured MAGST for each single loggers in the PERMOS network compared to the minimum and maximum Permafrost_cci MAGT at 0 m depth modelled in-between 2500 and 3000 m a.s.l. in the Swiss Alps. The measured in situ data range from around -7.5 °C to +7.5 °C, whereas Permafrost_cci MAGT ranges from around -1 °C to 4.5 °C. Only few loggers exhibit MAGST values greater than the modelled range, whereas many have lower MAGST.

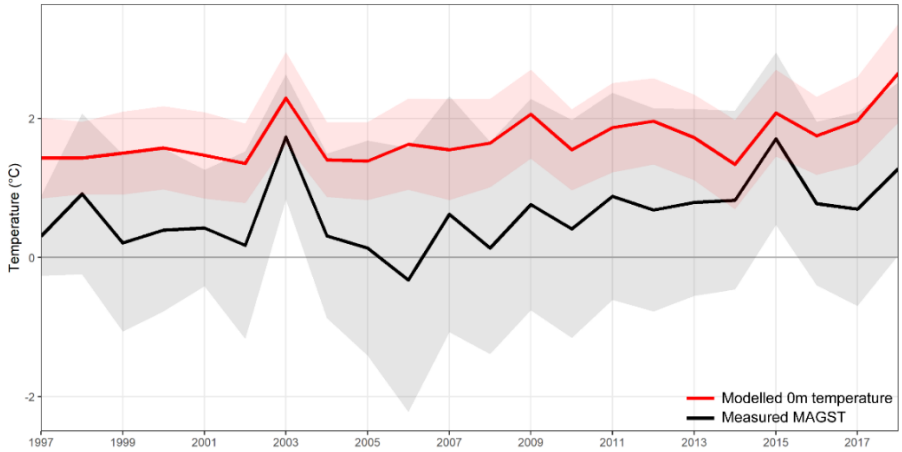

Figure 3.11. Temporal evolution of measured mean MAGST (black) and mean Permafrost_cci GTD POL at 0 m depth (red) over the entire Swiss Alps between 2500 and 3000 m a.s.l. The shaded area represent ± one standard deviation.

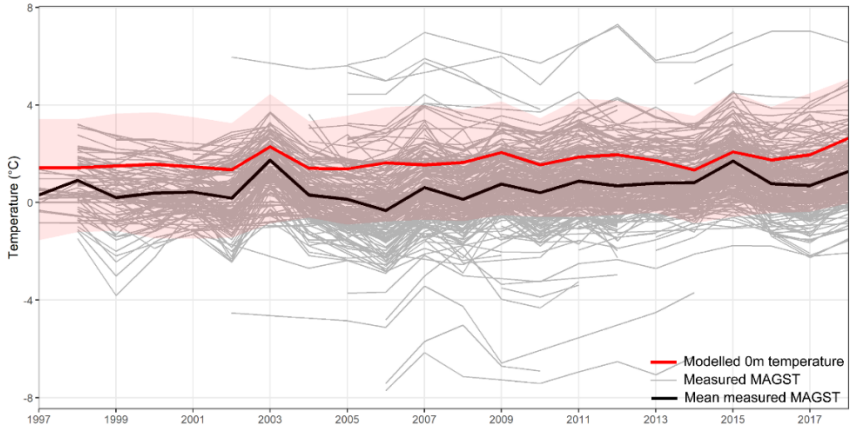

Figure 3.12. Temporal evolution of measured MAGST at all loggers in the Swiss Alps between 2500 and 3000 m a.s.l. (grey) compared to mean simulated Permafrost_cci GTD POL at 0 m depth (red). The shaded area represents the minimum and maximum GTD POL. The mean of all in situ measured sites is indicated in black.

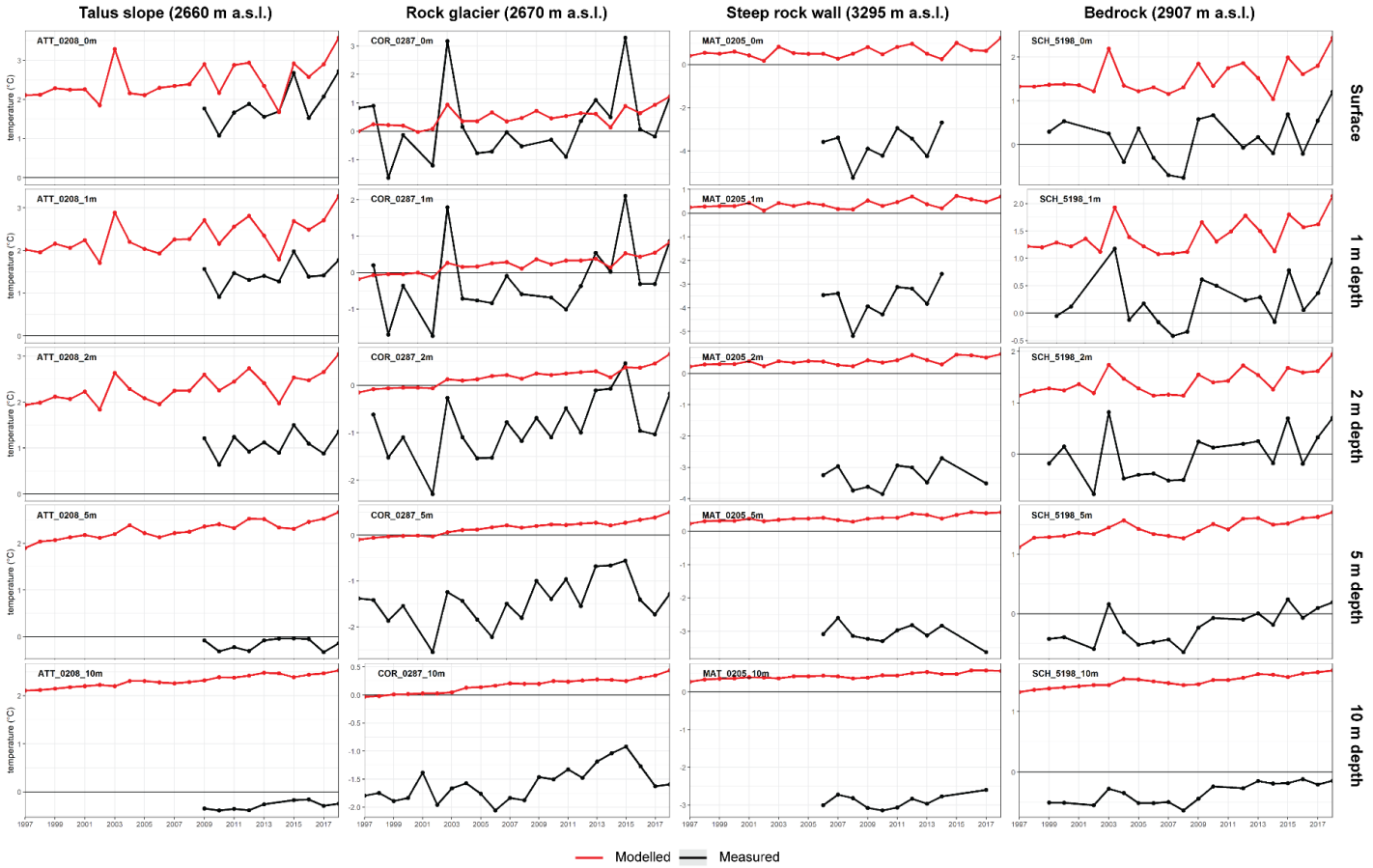

Figure 3.13. Comparison of simulated mean Permafrost_cci GTD POL (red) and in situ measured (black) MAGT at 0, 1, 2, 5 and 10 m depth at 4 sites in the Swiss Alps.

Comparing the modelled Permafrost_cci GTD POL at 0, 1, 2, 5 and 10 m depth to the in situ measured MAGT in boreholes (see Figure 3.14), Permafrost_cci GTD are systematically too warm at all depth and locations. The simulated Permafrost_cci GTD values fit better the in situ observations near the surface and the warm model bias increases with depth. The same pattern is found at all sites (Figure 3.14).

Although the absolute values are significantly different, both, the measured and the simulated MAGT, show a warming trend over the period 1997-2018. At depth, measured MAGT in 2017 show a more or less marked cooling effect. This is due to the extremely snow-poor winter 2016/17 in the Swiss Alps, which enabled the cold winter air temperature to cool more efficiently the ground (PERMOS 2019). This effect is not reproduced in Permafrost_cci simulations, illustrating the difficulty to include snow effects in global models.

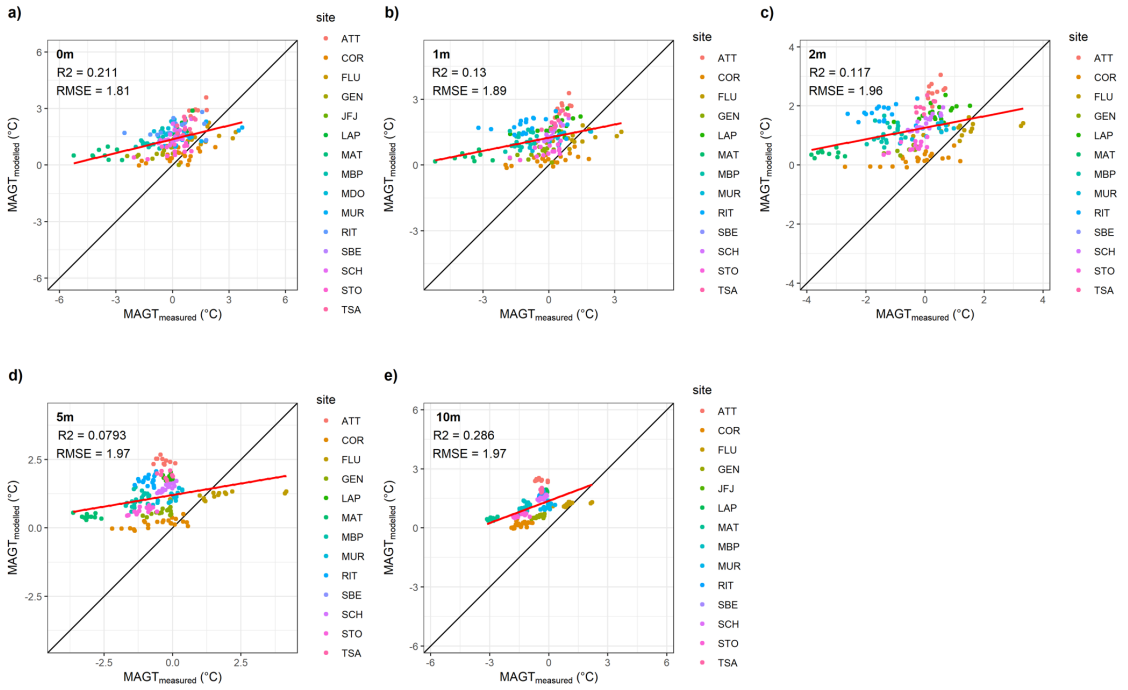

Figure 3.14. Comparison of simulated mean Permafrost_cci MAGT POL (y-axis) and in situ measured.

3.4 Permafrost_cci MAGT Comparison vs FT2T MAGT

A comparison of Permafrost_cci MAGT POL at 0 and 2 m depth with FT2T derived ground temperatures for selected locations demonstrate the expected higher variability of surface state from year to year, but also agreement of the different data sources regarding temperature level (Figures 3.15 & 3.16). Deviations can be found for sites in the transition zone (temperatures around 0°C) in Alaska as well as Russia. FT2T results are closer to in situ records than CRDPv1 at Svetlyy in Central Siberia and Boza Creek, Alaska (Figures 3.17 and 3.18). Specifically, Svetlyy is also discussed in section 5.1 as outlier location regarding permafrost extent evaluation. Results of CRDPv1 for Nadym, Western Siberia agree better with in situ then FT2T results. FT2T is too cold at this location. Here, the covered ASCAT footprint (appr. 12.5 km) contains a wide range of vegetation types (tundra shrubs to tall floodplain shrubs) and comparably wet soils. Either the Nadym borehole site is not representative for the footprint (but is for the 1km CRDv1 grid) or soil type/snow cover play an important role for heat transfer (insulation) which is not represented in the simple FT2T approach.

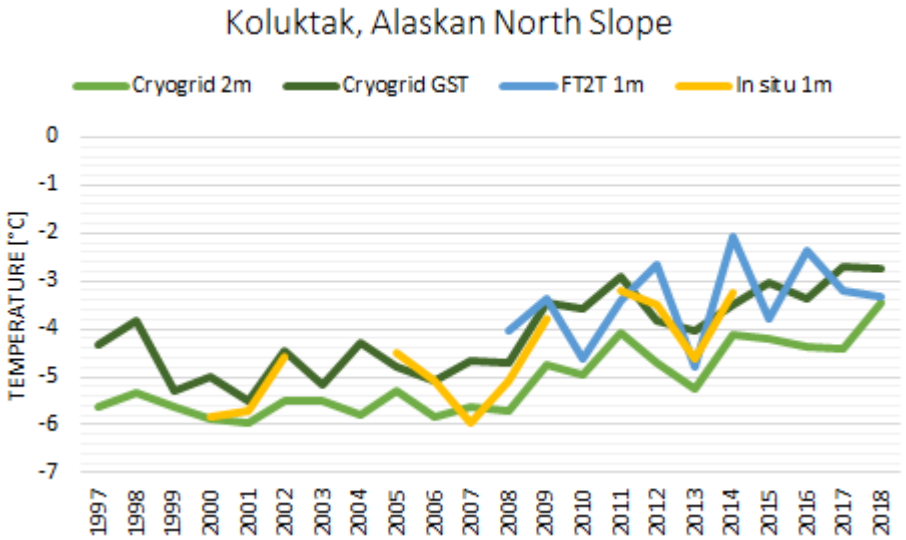

Figure 3.15. Comparison of FT2T product with CRDPv1 results and in situ data at Koluktak, Alaska.

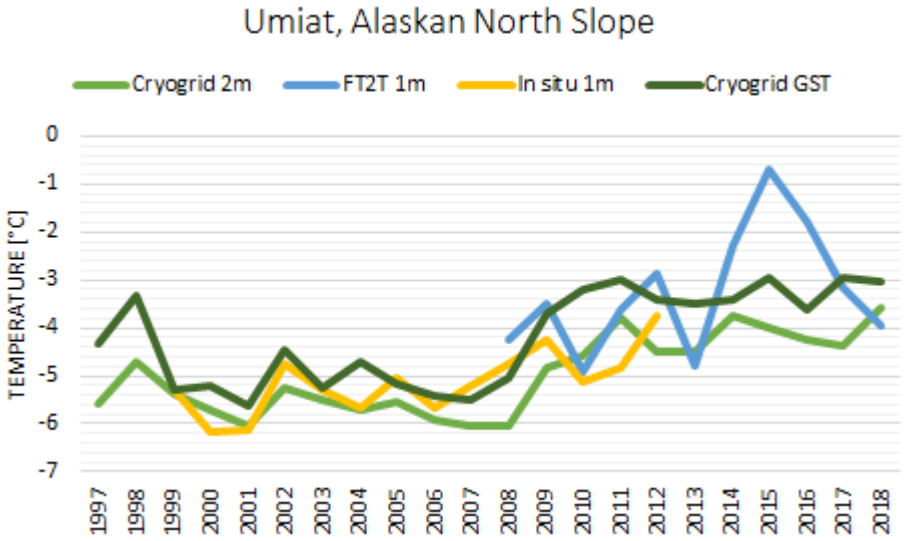

Figure 3.16. Comparison of FT2T product with CRDPv1 results and in situ data at Umiat, Alaska

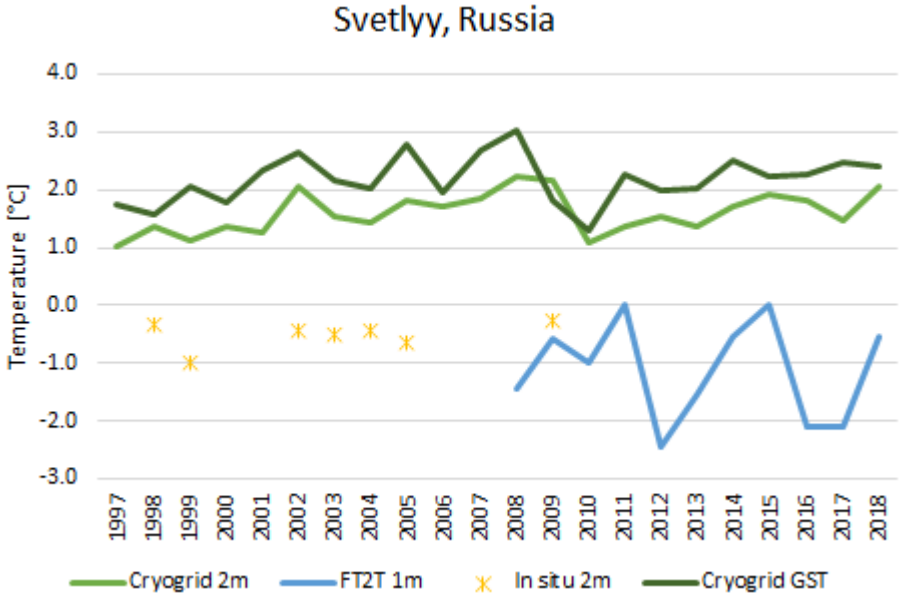

Figure 3.18. Comparison of FT2T product with CRDPv1 results and in situ data at Svetlyy, Central Siberia, Russia. See also permafrost extent discussion in section 5.1 and figure 5.6.

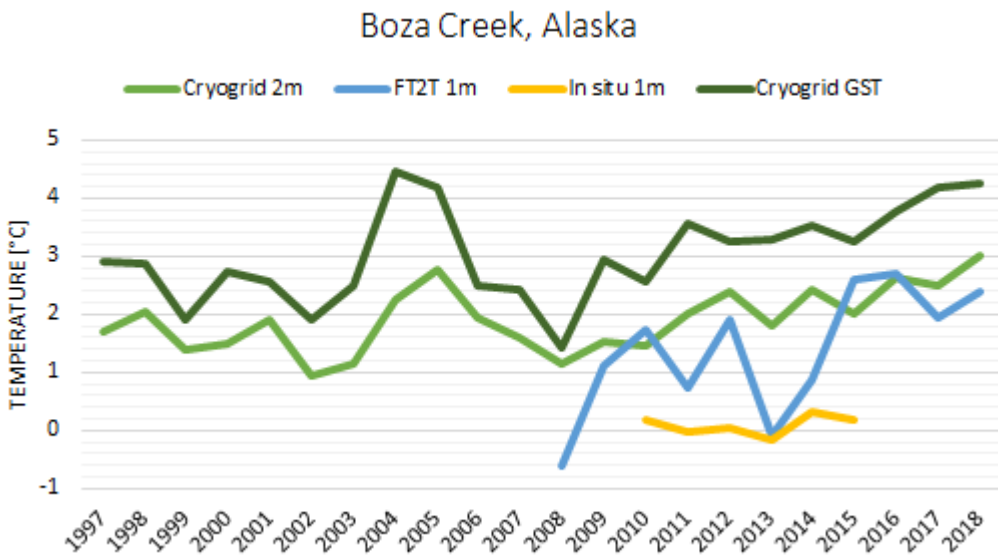

Figure 3.19. Comparison of FT2T product with CRDPv1 results and in situ data at Boza Creek, Alaska

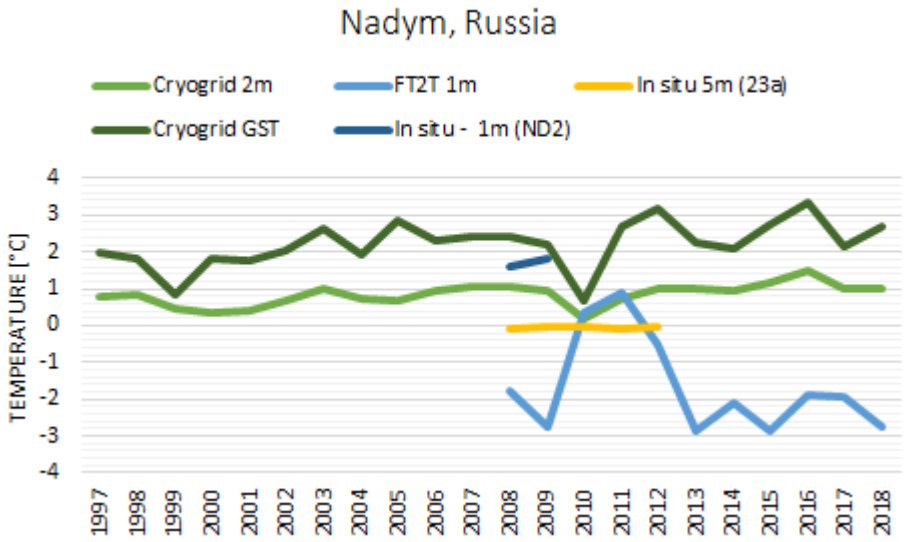

Figure 3.20. Comparison of FT2T product with CRDPv1 results and in situ data at Nadym, Western Siberia, Russia

4 ASSESSMENT RESULTS: ACTIVE LAYER THICKNESS

4.1 Active Layer Thickness User Requirements

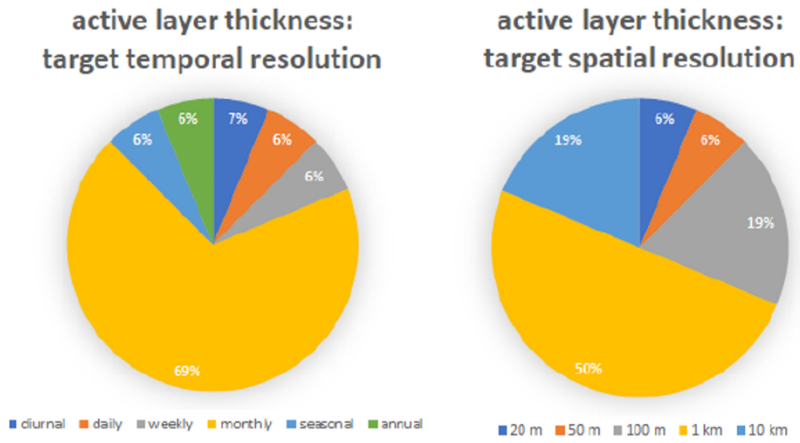

Figure 4.1. User Survey results. ESA CCI Permafrost User Survey results, Figure 4 [RD-4].

Users of potential products of active layer thickness are interested in high temporal resolution: monthly or higher in [RD-4]. Finally, less than 10% of users rated annual resolution as adequate as target temporal resolution in [RD-4]. However, the definition of the official ECV ALT is that it is the maximum thaw depth in summer and has by this the maximum temporal resolution of one year. Like this, the CRDP Permafrost_cci with ALT in annual resolution is the highest temporal resolution possible for this Permafrost ECV. Users were interested in higher temporal resolution, the representation of thaw depth that is developing deeper throughout the summer season until reaching the maximum depth in late summer, the ALT. But seasonal thaw depth evolution but is not considered an ECV (see also glossary in section 1.7). Half of the user group are satisfied with a target spatial resolution of 1 km. The 1^{rst} release of the Permafrost_cci CRDPv0 ALT provided annual resolution with the required 1×1 km spatial resolution from 2003 to 2017. The 2nd release Permafrost_cci CRDPv1 ALT provides annual resolution with the required 1×1 km² spatial resolution with a longer time span from 1997 to 2018.

4.2 Permafrost_cci ALT Match-Up Analyses with In Situ Data

For each in situ point location, the pixel in Permafrost_cci SIN and Permafrost_cci POL products closest to the in situ measurement was extracted to produce the match-up data set and derive statistics. Statistics were calculated comparing two matrices each: i) CRDP v1 Permafrost_cci ALT SIN and POL per year and ii) in situ ALT matching pixel-based pair-wise per station the same year.

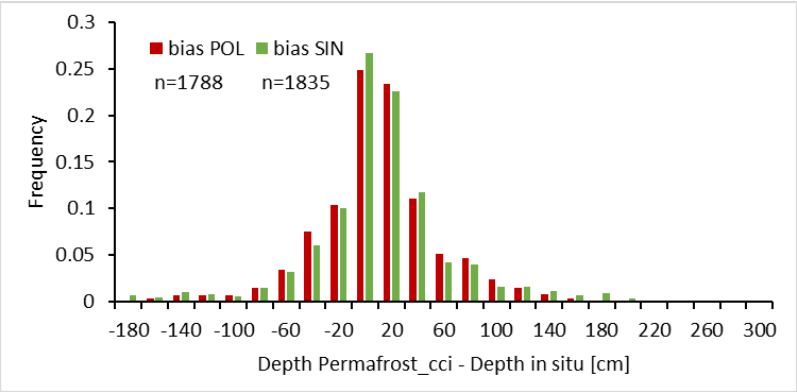

Figure 4.2. Frequency distribution of Permafrost_cci ALT SIN and POL minus in situ ALT. Without ALT Match-up data pairs from Mongolia, Central Asia, China, and the Siberian Yedoma (shape file of Bryant et al., 2017).

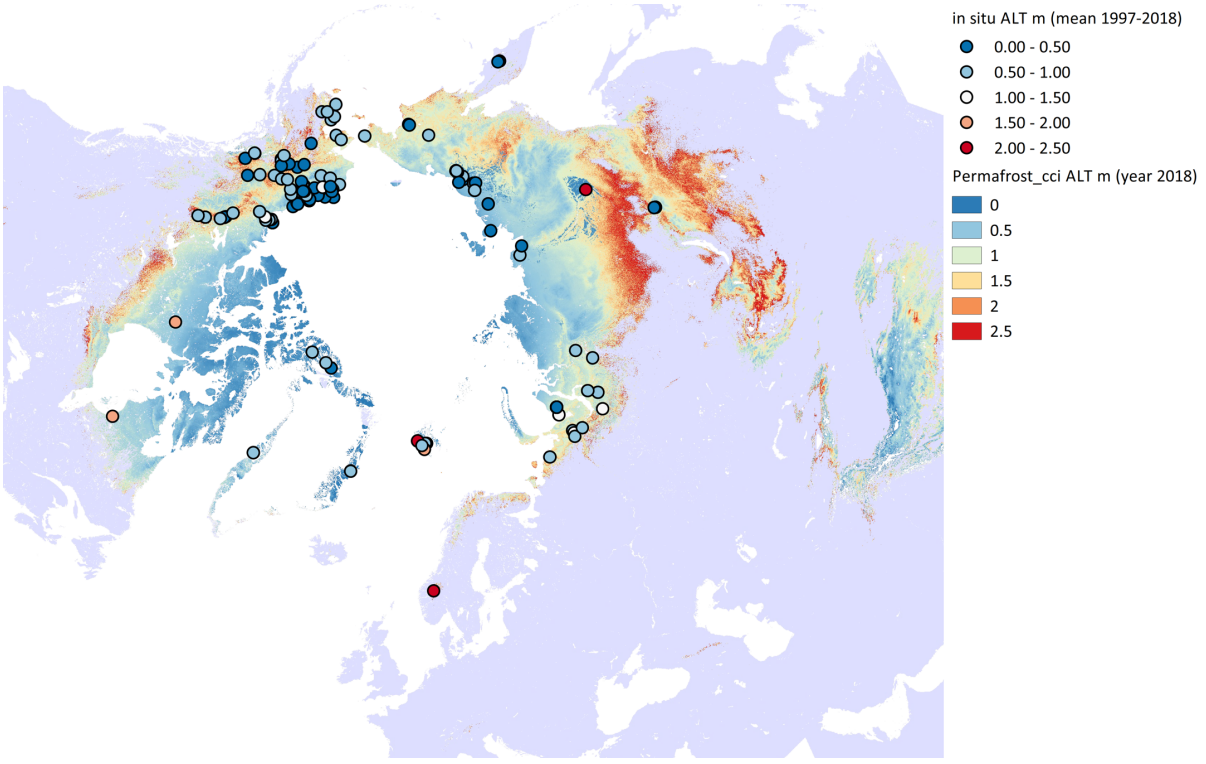

Figure 4.3. Sites included in the Permafrost_cci ALT Match-up analyses. Colours of site represent in situ ALT in m.

Table 4.1. Bias, absolute bias and root mean square RMSE of active layer thickness ALT (m) Without ALT Match-up data pairs from Mongolia, Central Asia and China and the Siberian Yedoma (shape file of Bryant et al., 2017) for Permafrost_CCI ALT mean SIN and POL.

	POL	**SIN**
bias_abs (m)	0.34	0.36
RMSE (m)	0.49	0.54

Table 4.2. Relative percentage error (RPE) and absolute percentage error (APE) for Permafrost_cci ALT SIN and POL. Without ALT Match-up data pairs from Mongolia, Central Asia, China, and the Siberian Yedoma (shape file of Bryant et al., 2017).

	SIN				POL			
	RPE (%)	RPE_{5-95} (%)	APE (%)	APE_{5-95} (%)	RPE (%)	RPE_{5-95} (%)	APE (%)	APE_{5-95} (%)
mean	17.75	9.52	52.32	43.41	17.01	9.70	51.06	43.24
sd	78.54	50.76	61.20	40.86	78.10	49.70	61.49	31.89
5% Quantile	-69.14		3.45		-65.92		-70.80	
95%Quantile	184.96		184.96		158.97		-77.87	

Table 4.3. Relative percentage error (RPE) and absolute percentage error (APE) for Permafrost_cci ALT SIN and POL per latitudinal range. Without ALT Match-up data pairs from Mongolia, Central Asia, and China and the Siberian Yedoma (shape file of Bryant et al., 2017).

	SIN				POL			
Latitude	RPE (%)	RPE_{5-95} (%)	APE (%)	APE_{5-95} (%)	RPE (%)	RPE_{5-95} (%)	APE (%)	APE_{5-95} (%)
54								
56	129.45	86.97	129.45	86.97	153.54	95.06	153.54	95.06
58	160.38	82.41	182.54	119.35	206.77	-38.43	222.14	38.43
60								
62	-8.07	1.76	55.70	55.70	-13.37	-1.10	50.39	50.39
64	110.74	54.04	121.03	69.83	120.83	55.96	131.12	70.91
66	90.43	56.66	99.49	68.67	74.45	53.73	83.55	64.20
68	56.17	30.02	67.96	46.50	50.14	33.11	60.89	50.08
70	1.97	2.45	30.67	32.53	0.18	1.07	33.34	35.00
72	-15.45	-15.28	28.08	30.36	-15.05	-14.45	28.11	30.25
74	-14.32	-9.76	15.52	15.52	-9.76	-9.76	11.05	11.05
78	-70.80	-64.30	70.80	70.80	-70.80	-62.50	70.80	70.80
80	-77.87	-58.47	77.87	77.87	-63.92	-15.41	64.18	65.64

Table 4.4. Relative percentage error (RPE) and absolute percentage error (APE) for Permafrost_cci ALT SIN and POL per in situ ALT (in cm). Without ALT Match-up data pairs from Mongolia, Central Asia, China, and the Siberian Yedoma (shape file of Bryant et al., 2017).

ALT	RPE POL	APE POL	RPE SIN	APE SIN
20				
40	36.57	36.57	36.57	36.57
60	37.87	37.87	37.87	37.87
80	16.30	16.30	16.30	16.30
100	-10.44	-10.44	-10.44	-10.44
120	-40.98	-40.98	-40.98	-40.98
140	-35.86	-35.86	-35.86	-35.86
160	-48.00	-48.00	-48.00	-48.00
180	-61.00	-61.00	-61.00	-61.00
200	-62.57	-62.57	-62.57	-62.57
220	-44.77	-44.77	-44.77	-44.77
240	-52.72	-52.72	-52.72	-52.72
260	-72.45	-72.45	-72.45	-72.45

Table 4.5. Bias, absolute bias and RMSE for Permafrost_cci ALT SIN and POL per in situ ALT (in cm). Without ALT Match-up data pairs from Mongolia, Central Asia, and China and the Siberian Yedoma (shape file of Bryant et al., 2017).

	POL				SIN			
ALT	bias	abs_bias	RMSE	n	bias	abs_bias	RMSE	n
20								
40	12.72	20.68	38.99	262	11.60	19.96	32.75	264
60	18.69	26.42	41.02	738	19.81	28.72	46.04	752
80	11.15	34.14	48.88	359	13.80	33.45	50.70	366
100	-9.99	38.19	47.85	179	-6.48	35.44	46.38	181
120	-45.38	47.82	53.21	113	-39.95	45.98	51.30	114
140	-47.42	48.22	56.53	50	-47.51	48.31	56.78	50
160	-72.48	72.48	78.44	31	-73.73	73.73	80.07	31
180	-105.37	105.37	116.29	22	-110.78	110.78	120.88	25
200	-119.42	120.20	129.66	14	-132.67	133.22	140.70	20
220	-93.13	93.13	97.70	14	-128.67	128.67	138.03	23
240	-121.20	121.20	125.24	5	-149.68	149.68	156.13	8
260	-177.50	177.50	177.50	1	-177.50	177.50	177.50	1

The error distribution Permafrost_cci ALT SIN and POL minus in situ CALM ALT is Gaussian, allowing statistics with ordinary least square metrics to estimate the deviation from the simulated Permafrost_cci variable values to the measured in situ values (Tables 4.1 to 4.5). However, scattergrams of Permafrost_cci ALT versus in situ ALT (Figure 4.4) show considerable deviation from the 1:1 best fit in both directions: under- and overestimation of ALT. The linear dependencies of over- and underestimation of ALT POL and SIN are geographically occurring at both, high latitudes and more southern latitudes. ALT POL and SIN perform worst at high latitudes and at the southern boundaries of permafrost zones. Match-up Analyses with data pairs from Mongolia, central Asia and the Tibetan Plateau (China) were excluded due to problematic performance and unknown reliability of in situ ALT data sets. A large proportion of the Match-up data set shows that Permafrost_cci ALT POL and SIN underestimate in situ ALT. This underestimation specifically occurs at high latitudes in polar desert regions without organic layer and vegetation insulation (Spitsbergen, Greenland) that have high in situ ALT despite cold air temperatures. Another large proportion of the Match-up data set shows that Permafrost_cci ALT POL and SIN overestimate in situ ALT. This overestimation seems to be characteristic for the southern boundaries of permafrost zones (e.g. Alaska, Canada).

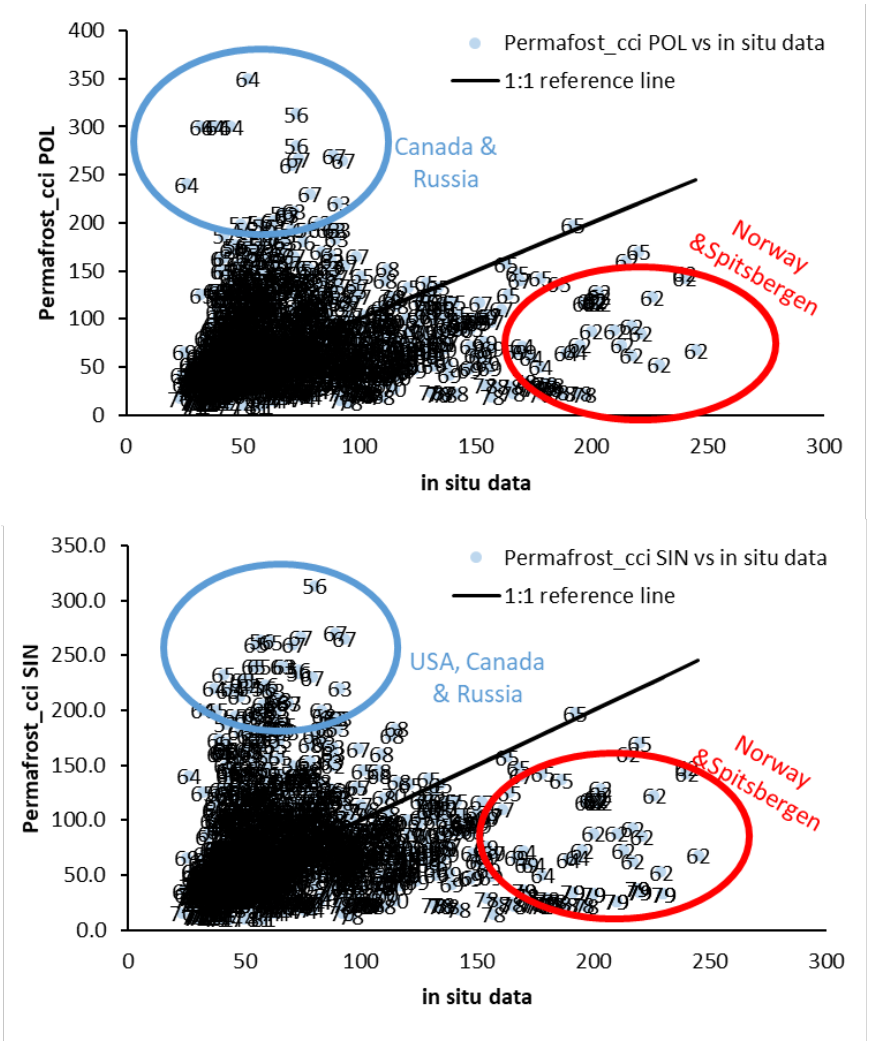

Figure 4.4. Regression of x = in situ ALT vs y= Permafrost_cci ALT SIN and POL. x = in situ ALT, y= Permafrost_cci ALT, all in cm. Labels = Latitude.

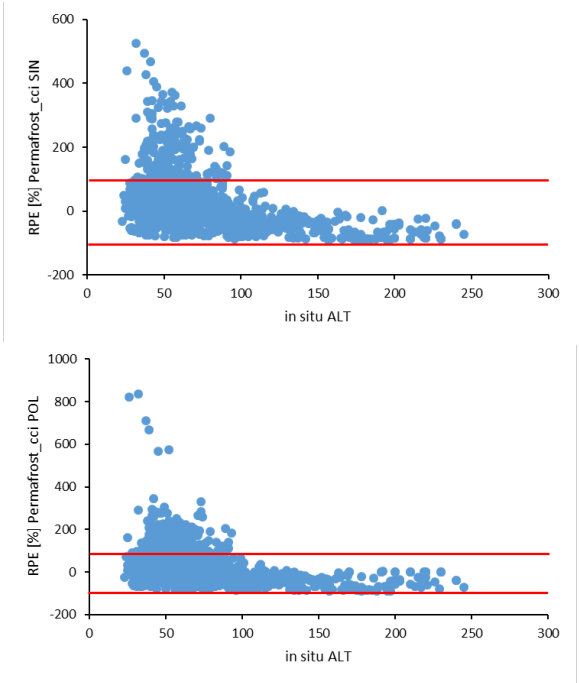

Figure 4.5. ALT in situ (cm, x-axis) versus relative error Permfrost_cci ALT POL/SIN RPE (y-axis). Red lines indicate the range of 100% uncertainty (relative percentage error).

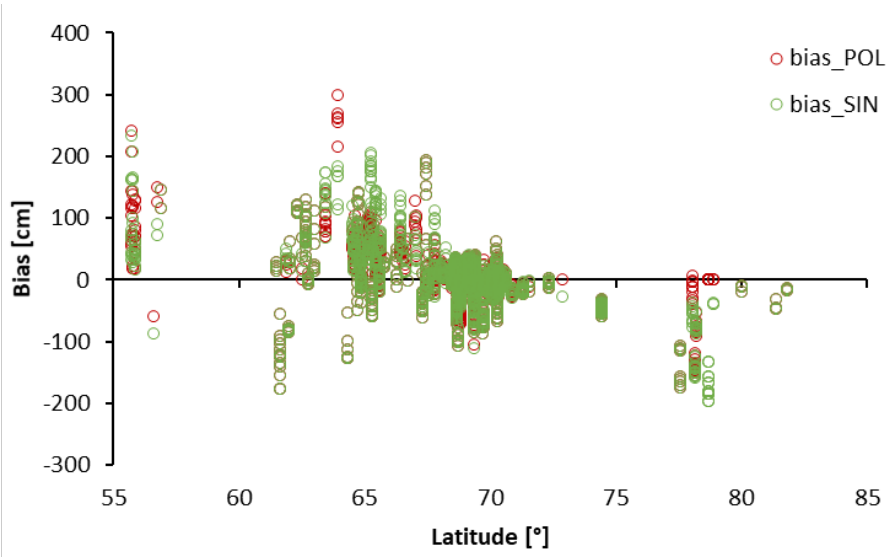

Figure 4.6. ALT bias of Permafrost_cci ALT SIN/POL (y-axis) per Latitude. n = 1835.

Match-up comparison to the ALT POL time series collection (1997 to 2018), in = 1835

Permafrost_cci ALT POL performance for in situ ALT (data from Mongolia, Central Asia and China and the Siberian Yedoma (shape file of Bryant et al., 2017) excluded is characterised by:

- an absolute bias of ~ 0.35 m and a RMSE of ~ 0.49 m
- a relative percentage error of ~ 10% (within the 5 to 95% Quantile), absolute percentage error ~ 44% (within the 5 to 95% Quantile).

Case 1 type deviation from 1:1:
Permafrost_cci ALT POL and SIN overestimate in situ ALT
i) Arctic rock and stone desserts in Svalbard and Greenland (e.g., Figure 4.4, 4.6)

Case 2 type deviation from 1:1:
Permafrost_cci ALT POL and SIN underestimate in situ ALT
ii) valley bottoms in mountain regions with shallow in situ ALT measured due to the fine-grained lithology but relatively warm in situ MAGT temperatures across all latitudes (with exception of the southern latitudes) and countries as this is a typical feature of Northern landscapes.
iii) at the southern boundaries of permafrost at mid-latitudes (e.g., Figure 4.6)

5 ASSESSMENT RESULTS: PERMAFROST EXTENT

5.1 Permafrost_cci PFR Match-Up Analyses with In Situ Data

Binary Match-up

Match-up with synthesised binary Permafrost Extent PFR (V1 2019)

Within the first validation round of CRDPv0 Permafrost_cci PFR we started with a preliminary binary match-up assessment as the group of 'non-permafrost temperature' CRDPv0 Permafrost_cci MAGT >1 °C was erroneous [RD-7].

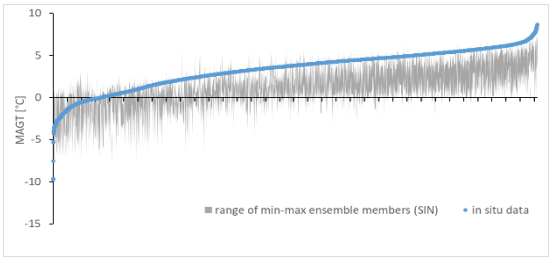

*In situ data MAGT (depths ≥40 cm) (blue points) and Permafrost*_cci CRDP v0 MAGT SIN min to from 5 ensemble members (grey-*shaded)* [RD-7].

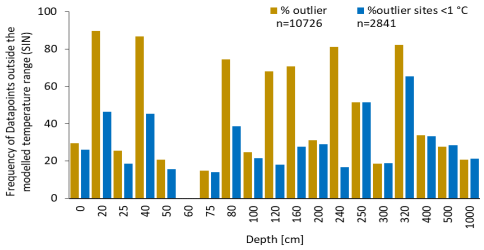

In situ MAGT (in %) outside of min max Permafrost_cci CRDP v0 MAGT SIN ensemble members. golden bars all sites, blue bars in situ MAGT <1 °[RD-7].*).*

We were, however successful with applying a large-scale regional assessment and therefore, allowed a small variability around MAGT 0 °C not setting "permafrost" strictly as in situ MAGT <0 °C in 2 consecutive years. This approach in [RD-7] was successful and we applied it more in depth for the assessment of CRDPv1 Permafrost_cci PFR.

Match-up with synthesised binary Permafrost Extent PFR (V2 2020)

We compare simulated Permafrost_cci MAGT SIN to in situ MAGT at all depths ≤1000 cm, analysing the amount of simulated and measured temperatures being both ≤0.5 °C ("permafrost") or both >0.5 °C ("no permafrost", Table 5.1). We analyse the complete data set (Mountain, Yedoma and landscape-anomaly-sites removed) and additionally the "warm" (MAGT >0 °C) and the "cold" (MAGT <1 °C) temperature groups.

Table 5.1. Accuracy for Permafrost_cci MAGT SIN. n (true) = data points with same Permafrost-classification in situ and simulated, n (false) = data points with different Permafrost classification.

	n (true)	n (false)	Accuracy
bulk data set	12272	1423	0.90
MAGT <1 °C	2873	313	0.90
MAGT >0 °C	9715	1277	0.88

For the assessment of Permafrost_cci PFR POL and SIN performance (in 0, 14, 29, 43, 57, 71, 86 or 100%) per site and year against in situ MAGT we use two approaches that we name case 1 and case 2. In case 1, we use the PFR permafrost probability grid-cell threshold of 0% as 'true no permafrost'. In case 2, we investigate the comparison with a threshold of Permafrost_cci PFR permafrost probability ≤40% as "no permafrost" (Table 5.3). For this binary assessment, we assign all in situ MAGT data to the group "permafrost" if

i) in any of the measurement depths from 0 to 240 cm within the years of 1997 to 2018 MAGT ≤0.5 °C and

ii) if in any of the measurement depths from 160 to 240 cm, within the years of 1997 to 2018, MAGT ≤0.5 °C was measured.

Accuracy calculates how many data points are considered as "permafrost" or "no permafrost" in both, in situ-derived "permafrost" or "no permafrost" and Permafrost_cci PFR POL derived "permafrost" or "no permafrost".

Table 5.2. Accuracy for in situ MAGT and mean of 5 ensemble members of Permafrost_cci MAGT POL and SIN at depths of 0, 1, 2, 5 and 10 m. n (true) = data points with same Permafrost-classification in situ and simulated, n (false) = data points with different Permafrost classification.

	POL			**SIN**		
	n (true)	**n (false)**	**Accuracy**	**n (true)**	**n (false)**	**Accuracy**
bulk	677	136	0.83	702	111	0.86
MAGT<1	677	90	0.88	701	66	0.91
MAGT>0	51	75	0.40	52	74	0.41

	POL interpolated			**SIN interpolated**		
	n (true)	**n (false)**	**Accuracy**	**n (true)**	**n (false)**	**Accuracy**
bulk	819	167	0.83	844	142	0.86
MAGT<1	819	105	0.89	843	81	0.91
MAGT>0	104	106	0.50	105	105	0.50

Table 5.3. Accuracy of Permafrost_cci PFR POL for Permafrost probability >0 and >40% considered as 100% permafrost for comparison with in situ data. Comparison conducted for any depth between 0 and 240 cm and for depths between 160 and 240 cm.

		Accuracy Case 1: PE>0	Accuracy Case 2: PE>40	n
i) 0-240 cm	all sites	0.64	0.86	3415
	MAGT <1 °C	**0.97**	0.96	833
	MAGT >0 °C	0.54	0.83	2709
ii) 160-240 cm	all sites	0.55	0.83	2583
	MAGT <1 °C	**0.95**	0.93	268
	MAGT >0 °C	0.51	0.82	2407

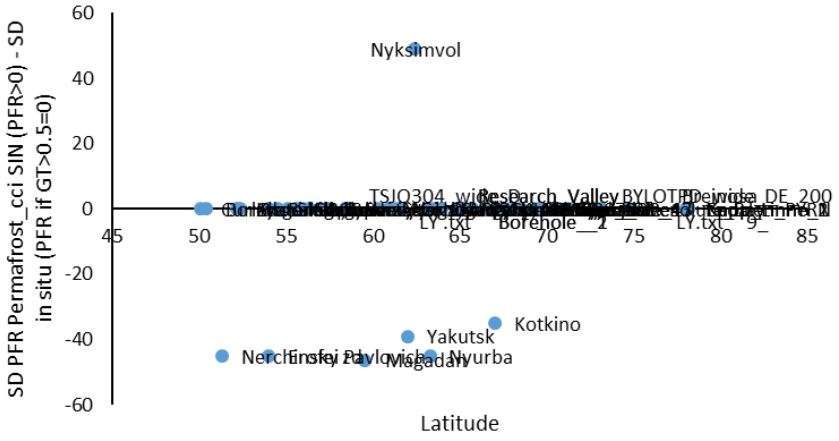

Figure 5.1. Comparison of standard deviations per site for all sites. Permafrost_cci PFR SIN permafrost probability versus in situ MAGT-derived permafrost probability: status between 160 and 240 cm set to 100% if in situ MAGT≤0.5 °C and set to 0 if in situ MAGT>0.5 °C.

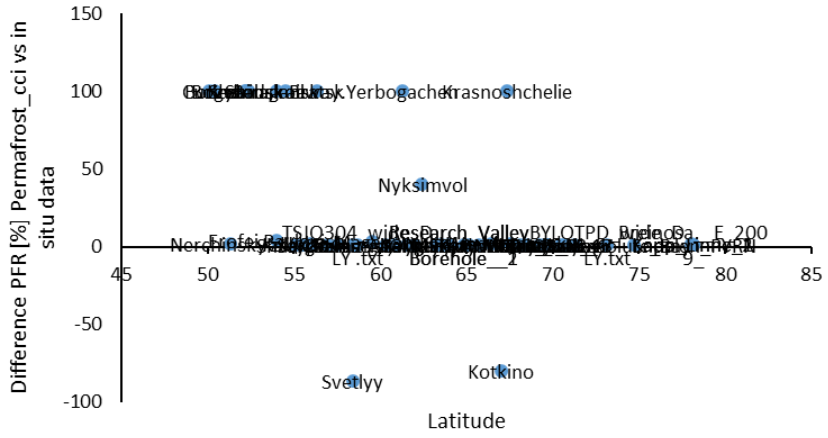

Figure 5.2. Mean PFR of Permafrost_cci SIN / PFR in situ (PFR=100 if min GT in 160-240 cm ≤0.5 °C). As division with 0 is not possible, Permafrost_cci SIN value is used if PFR in situ = 0, and PFR in situ-1 is used if Permafrost_cci SIN = 0.*

Comparing the standard deviations of this binary Permafrost_cci PFR to binary in situ MAGT permafrost per site, we found a robust Match-up result with only few outliers (Figure 5.1). As a site can have an SD of 0 in situ and in Permafrost_cci, but still have opposite definitions on the existence of Permafrost, we additionally looked at the percentage of same classifications in Permafrost_cci vs. in situ MAGT. It is calculated as mean PFR of Permafrost_cci SIN (PFR=100 if PFR>0) / mean PFR in situ (PFR=100 if min GT in 160-240 cm ≤0.5 °C). As division with 0 is not possible, Permafrost_cci SIN value is used if PFR in situ = 0, and PFR in situ *-1 is used if Permafrost_cci SIN = 0. This approach results in slightly more outliers, only two of them negative.

To get more match-up data on PFR, we included ALT sites into our analyses. While it is not possible to define non-Permafrost areas out of these data, we defined all sites/years with an ALT ≤300 cm as PFR=100%.

Table 5.4. Accuracy for Permafrost_cci MAGT SIN & in situ ALT and Permafrost_cci MAGT SIN. n (true) = data points with same Permafrost-classification in situ and simulated, n (false) = data points with different Permafrost classification.

	Accuracy Case 1: PE>0	Accuracy Case 2: PE>40	n
POL	0.75	0.88	4294
SIN	0.73	0.88	4418

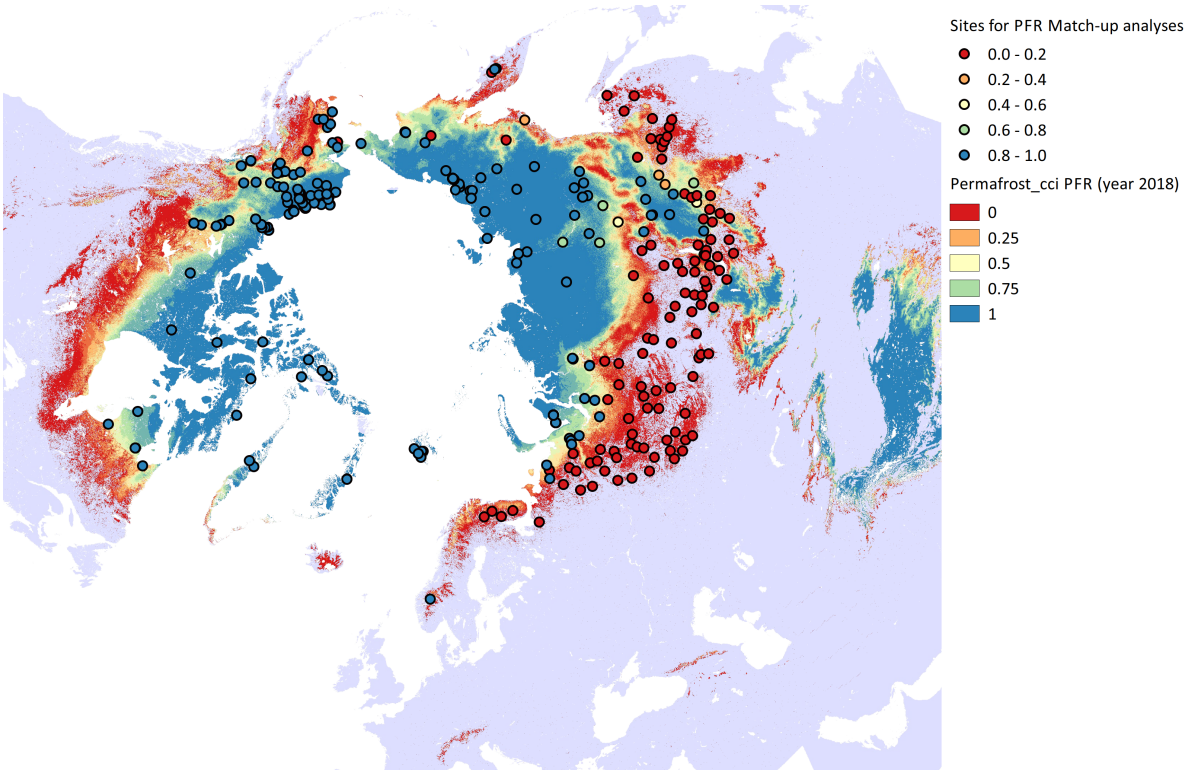

Figure 5.3. Sites for Permafrost_cci PFR Match-up analyses. Colours depict the fraction of years per site classified as Permafrost = yes (MAGT and ALT sites included).

Comparing the standard deviations of this binary Permafrost_cci PFR to binary in situ MAGT permafrost per site, we found a robust match-up result without outliers. As a site can have an SD of 0 in situ and in Permafrost_cci, but still have opposite definitions on the existence of Permafrost, we additionally looked at the percentage of same classifications in Permafrost_cci vs. in situ MAGT. It is calculated as mean PFR of Permafrost_cci SIN (PFR=100 if PFR>0) / mean PFR in situ (PFR=100 if min GT in 160-240 cm ≤0.5 °C). As division with 0 is not possible, Permafrost_cci SIN value is used if PFR in situ = 0, and PFR in situ*-1 is used if Permafrost_cci SIN = 0. This approach results in one single outlier (site Svetlyy, Figure 5.4) for the match-up group with MAGT <1 °C.

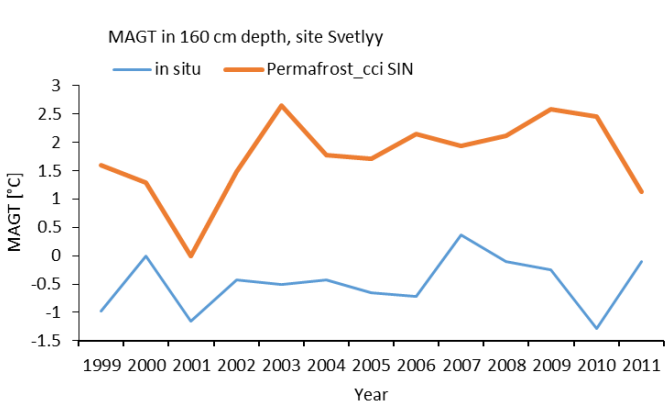

Figure 5.4. Permafrost_cci MAGT and in situ MAGT time series (1998 to 2011) in 1.60 m depth at RHM site Svetlyy (RU).

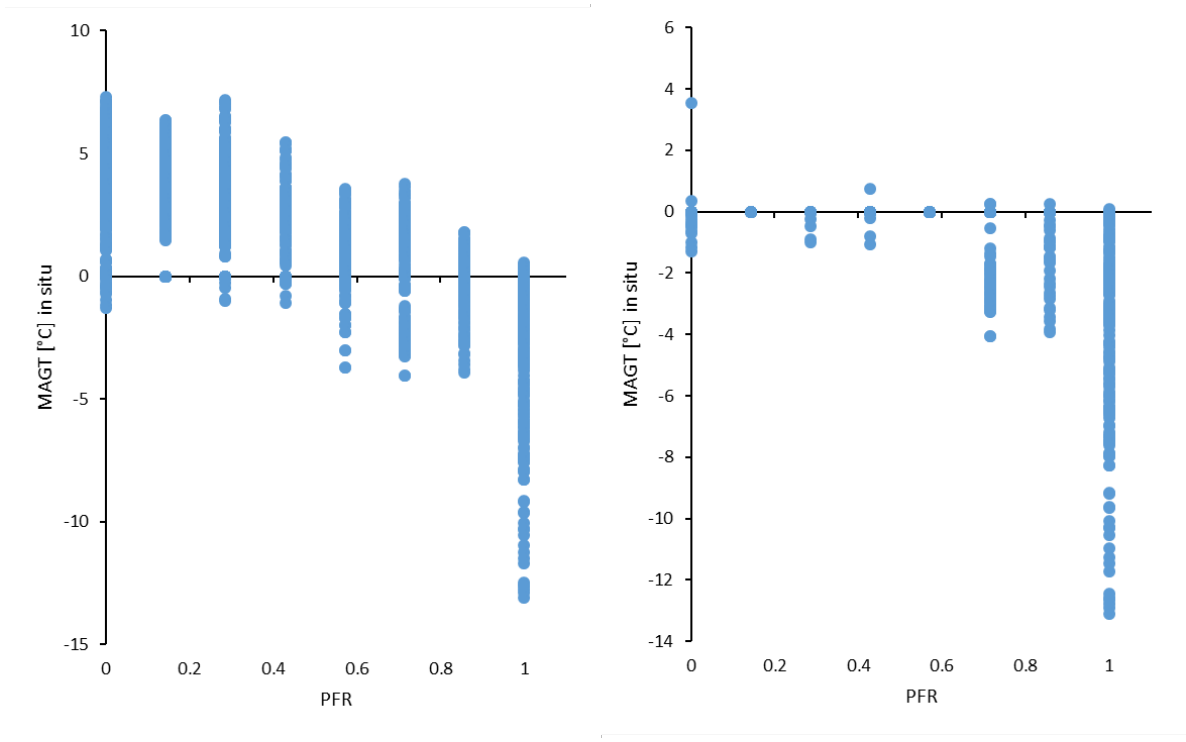

Figure 5.5. Match up of Permafrost_cci PFR permafrost probability SIN versus in situ MAGT (min MAGT between 160 - 240 cm depth) (left) for the bulk in situ MAGT match-up data set with pairs in time and (right) for sites with in situ MAGT <1 °C.

Permafrost_cci PFR POL performed best with the Match-up group of in situ MAGT <1 °C (Table 5.2, Figure 5.5, right). However, the binary Match-up of "permafrost" versus "no permafrost" for case 1, and case 2, for Permafrost_cci PFR permafrost probability vs. in situ MAGT ranges shows that depth-independent, **PFR permafrost probability in the grid cell is overestimated compared to in situ-derived "no permafrost" and MAGT ≤0.5 °C.**

Permafrost_cci PFR permafrost probability in the grid cell >0% occurs together with a wide range of "warm" in situ MAGT >0 °C (e.g., Figure 5.5, left). For example, a large fraction of Permafrost_cci PFR permafrost probability grid cells >60% occur together with an in situ MAGT range from 0 to 5 °C occurring at regional scales that are already independent from pixel-scale heterogeneity.

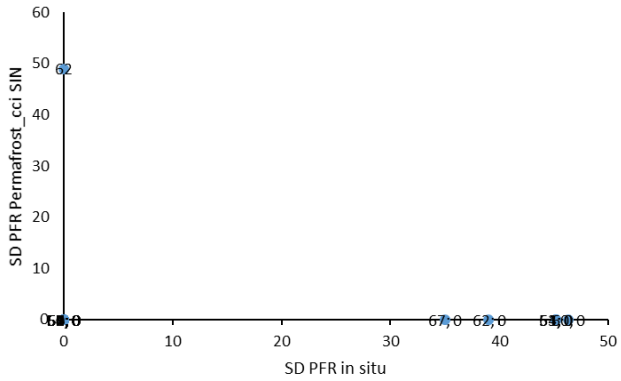

Figure 5.6. Comparison of standard deviations per site for sites with in situ MAGT >0 °C. Simulated probability of Permafrost_cci PFR POL: all values >0 set to 100. In situ data: minimum MAGT between 160 and 240 cm set to 100 if in situ MAGT ≤0.5 °C and set to 0 if in situ MAGT>0.5 °C. Labels are Latitudes.

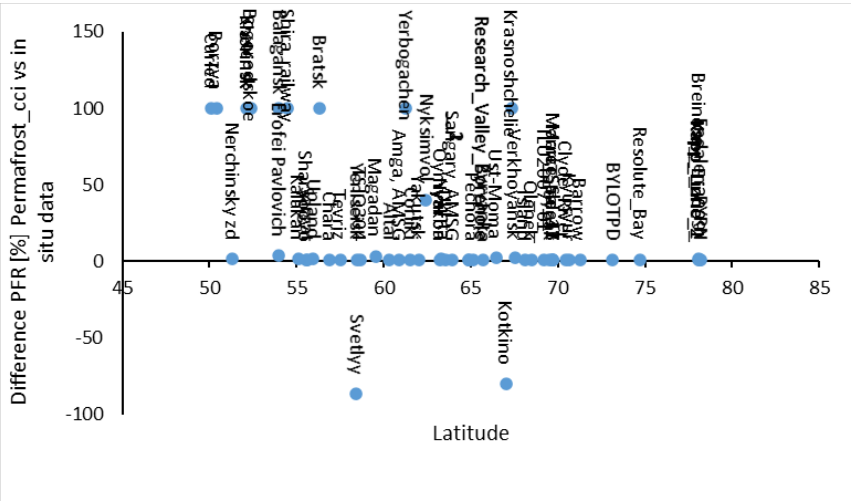

Figure 5.7. Comparison of standard deviations per site for sites with MAGT >0 °C. Simulated probability of Permafrost_cci PFR POL: all values >0% set to 100 %. In situ data: minimum GT between 160 and 240 cm set to 100 if in situ MAGT ≤0.5 °C and set to 0 if in situ MAGT>0.5 °C. Labels are station names.

The reason for too high simulated Permafrost_cci PFR permafrost probability at landscape scale is related to simulated too cold Permafrost_cci MAGT in the 'warm non-permafrost' temperature range.

5.4 PERMOS Permafrost Extent

Figure 5.10 compares the simulated Permafrost_cci MAGT mean at 10 m depth in 2015 in the Bas-Valais region with the slope movement inventory compiled for the same region within the ESA GlobPermafrost program. The red colour represents Permafrost_cci grid cells with MAGT at 10 m warmer than 0.2 °C in 2015, the blue colour Permafrost_cci grid cells with MAGT at 10 m colder than 0.2 °C in 2015 and the white colour MAGT between -0.2 and 0.2°C. The absence of colour-coded grid cells represent the areas not simulated by the model. One can clearly see that the extent of permafrost simulated by Permafrost_cci MAGT (i.e. MAGT <0 °C) is too restrictive. In the Swiss Alps, the lower limit of permafrost is usually found around 2600 m a.s.l. ± 200 m and within the simulated Permafrost_cci PE the lower limit is found around 3000 m a.s.l..

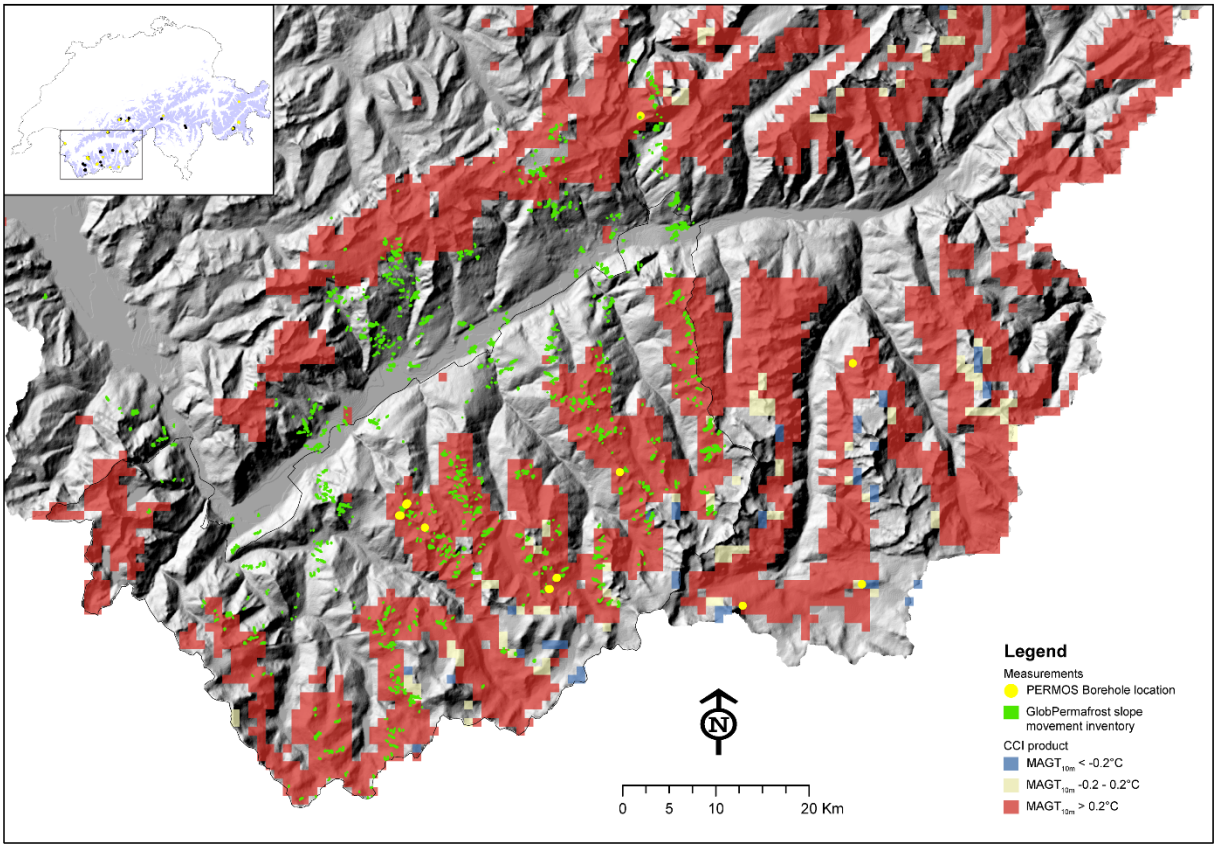

Figure 5.10. Overview of the simulated Permafrost_cci GTD at 10 m depth in 2015 in Bas-Valais (CH) compared to the ESA GlobPermafrost slope movement inventory and PERMOS permafrost monitoring borehole locations.

Furthermore, the vast majority of inventoried ESA GlobPermafrost slope movement products are located outside of the simulated Permafrost_cci permafrost extent area and only four amongst the 10 PERMOS permafrost borehole sites are located within the simulated Permafrost_cci PFR permafrost extent area (Table 5.7). Again, a clear warm bias in the simulated permafrost temperatures is observed in the Swiss Alps.

Table 5.5. Permafrost_cci PFR Permafrost probability (%) time series from 1997 to 2018 at the location of the PERMOS boreholes (Overview on GTN-P PERMOS boreholes in [RD-6], Table 4.4).

YEAR	ATT	COR	FLU	GEN	LAP	MAT	MPB	MUR	RIT	TSA	SCH	STO
1997	-	57	14	14	-	29	14	29	-	-	-	14
1998	-	57	14	14	-	29	14	29	-	-	-	14
1999	-	57	14	14	-	29	14	14	-	-	-	14
2000	-	57	14	14	-	29	14	14	-	-	-	14
2001	-	57	14	14	-	29	-	14	-	-	-	14
2002	-	57	14	14	-	29	-	14	-	-	-	14
2003	-	43	14	14	-	29	-	-	-	-	-	14
2004	-	43	14	14	-	29	-	-	-	-	-	14
2005	-	43	14	14	-	29	-	-	-	-	-	14
2006	-	43	14	14	-	29	-	-	-	-	-	14
2007	-	43	14	14	-	29	-	-	-	-	-	14
2008	-	43	-	14	-	29	-	-	-	-	-	29
2009	-	43	-	14	-	29	-	-	-	-	-	14
2010	-	43	-	14	-	29	-	-	-	-	-	14
2011	-	43	-	14	-	29	-	-	-	-	-	14
2012	-	43	-	14	-	14	-	-	-	-	-	14
2013	-	43	-	14	-	14	-	-	-	-	-	14
2014	-	43	-	14	-	14	-	-	-	-	-	14
2015	-	43	-	14	-	14	-	-	-	-	-	14
2016	-	43	-	14	-	14	-	-	-	-	-	14
2017	-	29	-	14	-	14	-	-	-	-	-	14
2018	-	29	-	14		14	-	-	-	-	-	14

6 SUMMARY

The growing demand for permafrost simulation products also needs to accommodate user requirements that span permafrost regions from Scandinavia, Mongolia, China to higher latitude permafrost in North America, Greenland, Siberia and all altitude ranges from lowland to mountain permafrost. This results in high difficulties of assessing how the products perform in all regions across a wide range of latitudes, altitudes, climate zones, land cover, and lithologies. This difficulty relies on inhomogeneous reference data sets in space, and time and challenging spatial scaling so that statistical match-up analyses with classical metrics are not easily interpreted or appropriate. RMSE provides an appropriate metric for validation when error distributions are Gaussian. In addition, metrics based on absolute deviations such as bias, relative percentage error, etc., are robust estimators. Ultimately, assessment results in Permafrost_cci will allow meaningful and constructive improvement in the accuracy of the derived ECV data products 'permafrost temperature', 'active layer thickness' as well as 'permafrost extent'.

Permafrost_cci retrieval skills are evaluated using pixel-based match-up analyses and additionally more complex combinations using expert knowledge. The validation and evaluation efforts also innovatively applied EO microwave-derived ground temperature, the Freeze-Thaw to Temperature (FT2T) product for comparison with the Permafrost_cci permafrost temperature product. GTN-P PERMOS in Switzerland is assessing the Permafrost_cci permafrost temperature and permafrost extent products in high-mountain permafrost regions, using in situ observations of surface temperature and borehole ground temperatures and the ESA GlobPermafrost rock glacier inventory on rock glaciers.

Permafrost_cci CRDPv1 provides 1 km pixel resolution ECV products on mean annual ground temperature (MAGT) at discrete ground depths (product name GTD), Active Layer Thickness (product name ALT) and Permafrost Fraction (product name PFR). All products are provided in Arctic stereographic circumpolar projection, that we name in this report the Permafrost_cci POL products. CRDPv1 is based on Permafrost_cci CryoGrid-3 runs using an ensemble of five models, providing Permafrost_cci CRDPv1 the GTD, ALT and PFR time series from 1997 to 2018 in annual resolution. Part of the MAGT and ALT Match-up analyses in this study are also carried out with the pre-release version in original sinusoidal projection based on MODIS tile format that are named in this report the Permafrost_cci MAGT and ALT SIN products. The Match-ups were executed using a pixel-based approach. Permafrost_cci MAGT SIN is provided in 0.0, 0.2, 0.25, 0.4, 0.5, 0.6, 0.75, 0.8, 1.0, 1.2, 1.6, 2.0, 2.4, 2.5, 3, 3.2, 4.0, 5.0, and 10.0 m depth, Permafrost_cci MAGT POL is provided for 0, 1, 2, 5, and 10 m depth.

The Permafrost_cci in situ reference data collections of MAGT and ALT are characterised by spatial and temporal biases in sampling related to regions, time covered, and measurement depths due to the high variety in national measurement programs, principal investigators and funding sources. This results in a large variability of Permafrost_cci reference in situ Match-up pairs in time, region, and, for example, MAGT reference depths. Permafrost_cci MAGT and ALT minus in situ MAGT and ALT frequency distributions are Gaussian. However, in situ MAGT and simulated Permafrost_cci MAGT data collections are characterised by bimodal and not Gaussian distributions.

The performance of Permafrost_cci MAGT for the bulk MAGT (including non-permafrost temperature) depth-time series using 13695 Match-up data pairs in time and depth is characterised by an absolute bias

of ~1.33 °C if calculated pairwise in the bulk data set, or an absolute bias of 1.43 °C if calculated in depth-specific data collections. The RMSE is 1.65 °C if calculated pairwise in the bulk data set, and 1.61 °C if calculated in depth-specific data collections. The relative percentage error within the 5 to 95% Quantile (thereby excluding the outliers, RPE_{5-95}) accounts for -17%, the absolute percentage error within the 5% to 95% Quantile (APE_{5-95}) is below 52%. Permafrost_cci MAGT is too cold at the southern rim of the permafrost zones and within the non-permafrost warm MAGT group.

We then confined the match-up evaluation to the data group of Match-up pairs built up from the in situ MAGT data collection <1 °C to focus on the permafrost temperature group. This Permafrost_cci MAGT SIN Match-up data set with pairwise depth- and time specific matching contains n = 3186 data pairs. Permafrost_cci MAGT SIN performance for all depths for in situ MAGT <1 °C is characterised by a warm bias of 1.05 °C and an absolute bias of 1.54 °C if calculated pairwise in the bulk data set, a warm bias of 0.95 °C and an absolute bias of 1.45 °C if calculated in depth-specific data collections. The RMSE is 1.85 °C if calculated pairwise in the bulk data set, and 1.73 °C if calculated in depth-specific data collections. The RPE_{5-95} accounts for 38%, the APE_{5-95} is 64%. The performance of Permafrost_cci MAGT SIN for all depths for the permafrost temperature group changed towards too warm estimates. This can be specifically observed for tundra sites in Alaska and Western Siberia.

The assessment of the Permafrost_cci POL product in 0, 1, 2, 5 and 10 m depths from 1997 to 2018 contains a Match-up data collection of 767 data pairs, increasing to 924 data pairs with interpolated data in shallow depths to fill in more data points at 1 m and 2 m depth. The addition of interpolated data slightly increases the Permafrost_cci POL performance. Permafrost_cci MAGT POL performance for all five depths for in situ MAGT <1 °C is characterised by a warm bias of 1.41 °C and an absolute bias of 1.63 °C if calculated pairwise in the bulk data set. The RMSE is 1.88 °C calculated pairwise in the bulk data set. The RPE_{5-95} accounts for 53%, the APE_{5-95} is 90%. The performance of Permafrost_cci MAGT POL for the five product depths for the permafrost temperature group shows an even warmer performance than the Permafrost_cci MAGT SIN data group for all depths down to 10 m. As the Match-up data collection for Permafrost_cci MAGT POL does not cover the RHM data set, these GTN-P tundra sites which are mainly located in Alaska and Western Yamal and are characterised by a strong warm bias become even more important for the overall performance metrics, worsening the performance of Permafrost_cci MAGT POL.

As a consequence of the cold bias in the warm temperature range, the binary match-up of “permafrost” versus “no permafrost” for Permafrost_cci PFR permafrost probability versus in situ MAGT ranges shows that PFR permafrost probability in the grid cell is overestimated compared to in situ-derived “no permafrost” and MAGT ≤0.5 °C. Permafrost_cci PFR permafrost probability in the grid cell >0% occurs together with a wide range of “warm” in situ MAGT >0 °C. A large fraction of Permafrost_cci PFR permafrost probability grid cells >60% occurs together with an in situ MAGT range from 0 to 5 °C occurring at regional scales that are already independent from pixel-scale heterogeneity.

PERMOS investigations in the Swiss Alps showed a too warm model bias of Permafrost_cci MAGT. The extent of permafrost simulated by Permafrost_cci PFR is too restrictive. In the Swiss Alps, the lower limit of permafrost is usually found around 2600 m a.s.l. ± 200 m and within the simulated Permafrost_cci PFR the lower limit is found around 3000 m a.s.l.. Furthermore, the vast majority of inventoried ESA GlobPermafrost slope movement products are located outside of the simulated

Permafrost_cci permafrost extent area and only four amongst the 10 PERMOS permafrost borehole sites are located within the simulated Permafrost_cci PFR permafrost extent area

Permafrost_cci MAGT >1 °C is systematically too warm at all depth and locations compared to in situ PERMOS MAGT. Permafrost_cci GTD values fit better the in situ observations near the surface and the warm model bias increases with depth at all sites. Although the absolute values are significantly different, both, the measured and the simulated MAGT, show a warming trend over the period 1997-2018. At depth, measured MAGT in 2017 show a more or less marked cooling effect. This is due to the extremely snow-poor winter 2016/17 in the Swiss Alps, which enabled the cold winter air temperature to cool more efficiently the ground. This effect is not reproduced in Permafrost_cci simulations, illustrating the difficulty to include snow effects in global models.

Ground temperatures based on satellite-derived freeze/thaw agree at selected cold sites for the overlap period 2008-2018. Deviations occur in the permafrost transition zone. In the presented cases, only one product (either CRDPv1 or FT2T) agrees with in situ measurements.

For the Permafrost_cci ALT Match-up analyses, we excluded all sites in Mongolia, Central Asia, on the Tibetan Plateau (China), and on the Siberian Yedoma. The characteristics of this Match-up data collection with 1835 Match-up pairs from 156 sites show a unimodal right-skewed distribution with a maximum around 0.40 to 0.80 m depth for Permafrost_cci POL; in situ CALM ALT shows maximum values in much shallower depths. However, Permafrost_cci ALT POL and SIN show an overrepresentation of shallow ALT values in the range of 0-20 cm and an underrepresentation at 60 cm, which is the most abundant class in the CALM in situ data set. Permafrost_cci ALT match-up shows a moderate absolute bias of ~0.35 m and RMSE of ~0.50 m if calculated for the bulk data collection, a relative percentage error of ~10% (within the 55 to 95% Quantile), and an absolute percentage error below 45%.

Linear regression of Permafrost_cci ALT versus in situ CALM ALT shows considerable deviation from the 1:1 best fit in both directions: under- and overestimation of ALT. Investigation of Permafrost_cci ALT shows a linear dependency on relative percentage error. One type of Permafrost_cci ALT underestimation of in situ ALT is linked to Arctic rock and stone desserts in Svalbard and Greenland. Permafrost_cci ALT overestimation of in situ ALT is linked to valley bottoms in mountain regions with shallow in situ ALT measured due to the fine-grained lithology but relatively warm in situ MAGT temperatures across all latitudes (with exception of the southern latitudes) as this is a typical feature of Northern landscapes. The Permafrost_cci ALT overestimation is also visible at the southern boundaries of permafrost at mid-latitudes.

7 REFERENCES

7.1 Bibliography

Allard, M., Sarrazin, D., L'Hérault, E. (2016): Borehole and near-surface ground temperatures in northeastern Canada, v. 1.4 (1988-2016). Nordicana D8, doi: 10.5885/45291SL-34F28A9491014AFD.

Bartsch, Annett; Pointner, Georg; Leibman, Marina O; Dvornikov, Yury; Khomutov, Artem V; Trofaier, Anna Maria (2017): Circumpolar ground-fast lake ice fraction by lake from ENVISAT ASAR late winter 2008, links to Shapefiles. PANGAEA, https://doi.org/10.1594/PANGAEA.873674, Supplement to: Bartsch, A et al. (2017): Circumpolar Mapping of Ground-Fast Lake Ice. Frontiers in Earth Science, 5(12), 16 pp, https://doi.org/10.3389/feart.2017.00012

Bergstedt, Helena; Bartsch, Annett (2020): Near surface ground temperature, soil moisture and snow depth measurements in the Kaldoaivi Wilderness Area, for 2016-2018. PANGAEA, https://doi.org/10.1594/PANGAEA.912482

Bergstedt, H., Bartsch, A., Duguay, C., Jones, B. (2020a). Influence of surface water on coarse resolution C-band backscatter: Implications for freeze/thaw retrieval from scatterometer data. Remote Sensing of Environment, 247, https://doi.org/10.1016/j.rse.2020.111911.

Bergstedt, H., Bartsch, A., Neureiter, A., Hofler, A., Widhalm, B., Pepin, N., & Hjort, J. (2020b). Deriving a frozen area fraction from Metop ASCAT backscatter based on Sentinel-1. IEEE Transactions On Geoscience And Remote Sensing, vol. 58, no. 9, pp. 6008-6019. https://doi.org/10.1109/tgrs.2020.2967364

Biskaborn, B. K.; Smith, S. L.; Noetzli, J.; Matthes, H.; Vieira, G.; Streletskiy, D. A.; Schoeneich, P.; Romanovsky, V. E.; Lewkowicz, A. G.; Abramov, A.; Allard, M.; Boike, J.; Cable, W. L.; Christiansen, H. H.; Delaloye, R.; Diekmann, B.; Drozdov, D.; Etzelmüller, B.; Grosse, G.; Guglielmin, M.; Ingeman-Nielsen, T.; Isaksen, K.; Ishikawa, M.; Johansson, M.; Johannsson, H.; Joo, A.; Kaverin, D.; Kholodov, A.; Konstantinov, P.; Kröger, T.; Lambiel, C.; Lanckman, J.-P.; Luo, D.; Malkova, G.; Meiklejohn, I.; Moskalenko, N.; Oliva, M.; Phillips, M.; Ramos, M.; Sannel, A. B. K.; Sergeev, D.; Seybold, C.; Skryabin, P.; Vasiliev, A.; Wu, Q.; Yoshikawa, K.; Zheleznyak, M., Lantuit, H. (2019): Permafrost is warming at a global scale. Nature Communications, 10, 264. https://doi.org/10.1038/s41467-018-08240-4

Biskaborn, B. K., Lanckman, J.-P., Lantuit, H., Elger, K., Streletskiy, D. A., Cable, W. L., and Romanovsky, V. E. (2015): The new database of the Global Terrestrial Network for Permafrost (GTN-P), Earth Syst. Sci. Data, 7, 245–259.

Boike, J., Nitzbon, J., Anders, K., Grigoriev, M. N., Bolshiyanov, D. Y., Langer, M., Lange, S., Bornemann, N., Morgenstern, A., Schreiber, P., Wille, C., Chadburn, S., Gouttevin, I., Kutzbach, L. (2018): Soil data at station Samoylov (2002-2018, level 1, version 1), link to archive. Alfred Wegener Institute - Research Unit Potsdam, PANGAEA, doi.org/10.1594/PANGAEA.891140

Brown, J., Ferrians Jr., O.J., Heginbottom, J.A., Melnikov, E.S. (1997). Circum-Arctic Map. of Permafrost and Ground-Ice Conditions. US Geological Survey Reston.

Bryant, R.N., Robinson, J.E., Taylor, M.D., Harper, William, DeMasi, Amy, Kyker-Snowman, Emily, Veremeeva, Alexandra, Schirrmeister, Lutz, Harden, Jennifer and Grosse, Guido, 2017, Digital Database and Maps of Quaternary Deposits in East and Central Siberia: U.S. Geological Survey data release, https://doi.org/10.5066/F7VT1Q89.

Center for Northern Studies in Canada, CEN (2013): Environmental data from Northern Ellesmere Island in Nunavut, Canada, v. 1.0 (2002-2012). Nordicana D1, doi.org/10.5885/44985SL-8F203FD3ACCD4138.

GTN-P (2018): GTN-P global mean annual ground temperature data for permafrost near the depth of zero annual amplitude (2007-2016). PANGAEA, https://doi.org/10.1594/PANGAEA.884711

Kroisleitner, C., Bartsch, A., and Bergstedt, H.: Circumpolar patterns of potential mean annual ground temperature based on surface state obtained from microwave satellite data, The Cryosphere, 12, 2349-2370, https://doi.org/10.5194/tc-12-2349-2018, 2018.

Naeimi, Vahid; Bartalis, Zoltan; Hasenauer, Stefan; Wagner, Wolfgang (2009): An improved soil moisture retrieval algorithm for ERS and METOP scatterometer observations. IEEE Transactions on Geoscience and Remote Sensing, 47(7), 1999-2013, https://doi.org/10.1109/TGRS.2008.2011617

Paulik, Christoph; Melzer, Thomas; Hahn, Sebastian; Bartsch, Annett; Heim, Birgit; Elger, Kirsten; Wagner, Wolfgang (2014): Circumpolar surface soil moisture and freeze/thaw surface status remote sensing products (version 4) with links to geotiff images and NetCDF files (2007-01 to 2013-12). Department of Geodesy and Geoinformatics, TU Vienna, PANGAEA, https://doi.org/10.1594/PANGAEA.832153

Wang, K. (2018): A synthesis dataset of near-surface permafrost conditions for Alaska, 1997-2016. Arctic Data Center, doi.org/10.18739/A2KG55.

7.2 Acronyms

ALT	Active Layer Thickness
APE	Absolute Percentage Error
AWI	Alfred Wegener Institute Helmholtz Centre for Polar and Marine Research
B.GEOS	b.geos GmbH
CALM	Circumpolar Active Layer Monitoring
CC1	GlobPermafrost CryoGrid 1
CC3	Permafrost_cci CryoGrid 3
CEN	Center for Northern Studies in Canada
CliC	Climate and Cryosphere project
CLM4	Land Community Model
CCI	Climate Change Initiative
CMIP-6	The Coupled Model Intercomparison Project
CMUG	Climate Modelling User Group
CRDP	Climate Research Data Package
ECV	Essential Climate Variable
EO	Earth Observation
ESA	European Space Agency
ESA DUE	ESA Data User Element
FT2T	Freeze-Thaw to Temperature
GAMMA	Gamma Remote Sensing AG
GCOS	Global Climate Observing System
GCW	Global Cryosphere Watch
GT	Ground Temperature
GTN-P	Global Terrestrial Network for Permafrost
GTOS	Global Terrestrial Observing System
GUIO	Department of Geosciences University of Oslo
IASC	International Arctic Science Committee
IPA	International Permafrost Association
IPCC	Intergovernmental Panel on Climate Change
MAGT	Mean Annual Ground Temperature
NetCDF	Network Common Data Format
NSIDC	National Snow and Ice Data Center
PE	Permafrost Extent
PERMOS	Swiss Permafrost Monitoring Network

PF	Permafrost
POL	POLar stereographic circum-arctic projection
PSTG	Polar Space Task Group
RD	Reference Document
RMSE	Root Mean Square Error
RPE	Relative Percentage Error
RS	Remote Sensing
SAR	Synthetic Aperture Radar
SCAR	Scientific Committee on Antarctic Research
SD	Standard Deviation
SIN	SINusoidal projection
SU	Department of Physical Geography Stockholm University
TSP	Thermal State of Permafrost
TTOP	Temperature at top of permafrost
UNIFR	Department of Geosciences University of Fribourg
URD	Users Requirement Document
WCRP	World Climate Research Program
WMO	World Meteorological Organisation
WMO OSCAR	Observing Systems Capability Analysis and Review Tool
WUT	West University of Timisoara